Research Article

Combined Effect of Proteasome and Calpain Inhibition on Cisplatin-Resistant Human Melanoma Cells

Izabela Młynarczuk-Biały,[1,4] Heike Roeckmann,[6] Ulrike Kuckelkorn,[1] Boris Schmidt,[7] Sumaira Umbreen,[7] Jakub Gołąb,[5] Antje Ludwig,[2] Christina Montag,[3] Lüder Wiebusch,[3] Christian Hagemeier,[3] Dirk Schadendorf,[6] Peter-M. Kloetzel,[1] and Ulrike Seifert[1]

[1]Institut fuer Biochemie Charité-Universitaetsmedizin Berlin; [2]Medizinische Klinik und Poliklinik, Schwerpunkt Kardiologie, Angiologie, Pneumologie Charité-Universitaetsmedizin; [3]Abteilung fuer Paediatrie, Labor fuer Molekulare Biologie, Charité-Universitaetsmedizin, Berlin, Germany; [4]Department of Histology and Embryology, Centre for Biostructure Research, The Medical University of Warsaw; [5]Department of Immunology, Centre for Biostructure Research, The Medical University of Warsaw, Warsaw, Poland; [6]Klinische Kooperationseinheit fuer Dermatoonkologie, Abteilung fuer Dermatologie, Universitaetsklinikum Mannheim, Mannheim, Germany; and [7]Clemens-Schoepf-Institute fuer Organische Chemie und Biochemie TU Darmstadt, Darmstadt, Germany

Abstract

Resistance of tumor cells to cisplatin is a common feature frequently encountered during chemotherapy against melanoma caused by various known and unknown mechanisms. To overcome drug resistance toward cisplatin, a targeted treatment using alternative agents, such as proteasome inhibitors, has been investigated. This combination could offer a new therapeutic approach. Here, we report the biological effects of proteasome inhibitors on the parental cisplatin-sensitive MeWo human melanoma cell line and its cisplatin-resistant $MeWo_{cis1}$ variant. Our experiments show that proteasome inhibitor treatment of both cell lines impairs cell viability at concentrations that are not toxic to primary human fibroblasts *in vitro*. However, compared with the parental MeWo cell line, significantly higher concentrations of proteasome inhibitor are required to reduce cell viability of $MeWo_{cis1}$ cells. Moreover, whereas proteasome activity was inhibited to the same extent in both cell lines, IκBα degradation and nuclear factor-κB (NF-κB) activation in $MeWo_{cis1}$ cells was proteasome inhibitor independent but essentially calpain inhibitor sensitive. In support, a calpain-specific inhibitor impaired NF-κB activation in $MeWo_{cis1}$ cells. Here, we show that cisplatin resistance in $MeWo_{cis1}$ is accompanied by a change in the NF-κB activation pathway in favor of calpain-mediated IκBα degradation. Furthermore, combined exposure to proteasome and calpain inhibitor resulted in additive effects and a strongly reduced cell viability of $MeWo_{cis1}$ cells. Thus, combined strategies targeting distinct proteolytic pathways may help to overcome mechanisms of drug resistance in tumor cells. (Cancer Res 2006; 66(15): 7598-605)

Introduction

Melanoma is a malignant neoplasia of melanoblastic origin that is the leading cause of death from cutaneous malignant disease (1). Thus far, in metastatic melanoma, single-agent chemotherapy, including dacarbazine, nitrosoureas, *Vinca* alkaloids, cisplatin, paclitaxel, and bleomycin, have not been proven to be beneficial, with response rates well below 25% and no demonstration of prolonged survival (2). Cisplatin is frequently part of polychemotherapy regimens in melanoma treatment based on the feature that cells deficient in DNA repair are hypersensitive to cisplatin (3). However, the presence or development of cisplatin resistance is an important clinical limitation. Mechanisms of cisplatin resistance are usually multifactorial and include enhanced efflux, oncogene overexpression, defects in apoptosis pathways, and can be affected by cisplatin-mediated induction of endoplasmic reticulum stress (4, 5). Alternative approaches are urgently needed. Thus, combination of conventional chemotherapeutics with novel biological agents, such as proteasome inhibitors, need to be studied carefully. In this context, proteasome inhibitors have been described that induce cell cycle arrest and apoptosis, and that could sensitize malignant cells to proapoptotic effects of conventional chemotherapeutics (6, 7). The target for proteasome inhibitors is the multicatalytic protease complex called proteasome, which degrades mostly ubiquitinated proteins in the cytosol and nucleus. Therefore, the proteasome system is involved in various pathways, such as regulation of transcription, apoptosis, and cell cycle. In transcriptional regulation, the proteasome also activates nuclear factor-κB (NF-κB) by degrading its inhibitory proteins (IκB). Stimulation of cells by tumor necrosis factor (TNF) results in the phosphorylation and subsequent proteasomal degradation of IκBα, which allows NF-κB to enter the nucleus. There, NF-κB regulates the expression of its target genes. In many tumor cells, prolonged NF-κB activation can lead to inhibition of apoptosis and therapeutic failure. Previous studies indicate that in this context, NF-κB could also be activated in a proteasome-ubiquitin-independent pathway due to calpain-dependent IκBα degradation (8). Calpains are nonlysosomal, calcium-dependent proteases that cleave a specific subset of cellular proteins, including cytoskeletal proteins, membrane receptors, and many transcription factors (9).

The aim of this study was to analyze the biological effects of proteasome inhibition in cisplatin-resistant and cisplatin-sensitive human melanoma cells. In particular, we examined cellular effects of a new proteasome inhibitor, BSc2118 (10). Our data show that proteasome inhibitor treatment of cisplatin-sensitive and cisplatin-resistant melanoma cells induces cell death at concentrations that are not toxic to primary human fibroblasts. Moreover, our data provide evidence that cisplatin-resistant cells are considerably more resistant to proteasome inhibition than parental

Note: Supplementary data for this article are available at Cancer Research Online (http://cancerres.aacrjournals.org/).

Requests for reprints: Peter-M. Kloetzel, Institut fuer Biochemie, Charité-Universitaetsmedizin Berlin, Monbijoustr.2, 10117 Berlin, Germany. Phone: 49-30450528232; Fax: 49-30450528921; E-mail: p-m.kloetzel@charite.de.

doi:10.1158/0008-5472.CAN-05-2614

cisplatin-sensitive melanoma cells. However, combined proteasome and calpain inhibition dramatically reduces the cell viability of $MeWo_{cis1}$ melanoma cells and helps to overcome the relative proteasome inhibitor resistance of these cells.

Materials and Methods

Materials. The proteasome inhibitors MG-132 (Calbiochem, Darmstadt, Germany), PS-341 (Millenium Pharmaceuticals, Ltd., Chiswick, United Kingdom), and BSc2118 (10) were dissolved in DMSO at a concentration of 10 mmol/L. Stock solutions of calpain inhibitors PD150606 (Calbiochem) and E64 (Sigma, St. Louis, MO) were prepared in DMSO at 100 mmol/L. BAY 11-7082 (Calbiochem), an inhibitor of TNF-induced IκBα degradation, was prepared in DMSO at 100 mmol/L. Cisplatin (Medac, Hamburg, Germany) was dissolved in FCS-free RPMI at 1 mg/mL and kept at −20°C. Recombinant mouse TNF-α (hereafter named as TNF; Roche, Mannheim, Germany) was stored at −20°C before use. The specific activity of TNF is 4×10^8 units/mg and this TNF is also effective on human cells.

Cell culture. MeWo and $MeWo_{cis1}$ cells were cultured in RPMI 1640 (Biochrom, Berlin, Germany) supplemented with 10% FCS, penicillin (100 units/mL), and streptomycin (100 μg/mL) as described (11). $MeWo_{cis1}$ cells were cultured with additional cisplatin at 1 μg/mL. Primary human fibroblasts (PromoCell GmbH, Heidelberg, Germany) were grown in fibroblast growth medium supplied by the manufacturer.

Cell proliferation assays. The cytotoxic/cytostatic effects of proteasome inhibitors on melanoma cells or human primary fibroblasts were examined *in vitro* using the crystal violet assay, as previously described (12). Briefly, 5×10^3 cells per well were seeded in 96-well microtiter plates in a total volume of 100 μL/well (Greiner) and proteasome inhibitor exposure was done the following day. Serial dilutions of MG-132, PS-341, and BSc2118 (final concentrations 0-1,000 nmol/L) were added in quadruplicates. After an incubation period of 24, 48, or 72 hours with proteasome inhibitors, cells were stained with 0.1% crystal violet (Sigma). Cytotoxic/cytostatic effect was expressed as relative viability of treated cells (percentage of control cells incubated with medium only) and was calculated as follows: relative viability = $(A_e - A_b) \times 100 / (A_c - A_b)$, where A_b is background absorbance, A_e is experimental absorbance, and A_c is the absorbance of untreated controls.

To assess drug sensitivity in melanoma cells, we also did colony growth assay using 96-well plates. Cells were plated at 20 per well and BSc2118 was used at the same concentrations as before. After 15 days of incubation, colonies were stained with crystal violet and were counted. BSc2118 treatment was done in quadruplicate at each concentration. The value obtained in wells treated with medium only was assigned as 100% of growth.

Protease activity assays in cell extracts and purified 20S proteasomes. Cells were seeded in 96-well plates at a density of 1×10^4 per well. After incubation with proteasome inhibitors (MG-132, PS-341, and BSc2118) from 0 to 1,000 nmol/L, cells were washed with PBS and lysed [20 mmol/L Tris-HCl (pH 6.8), 50 mmol/L NaCl, 2 mmol/L $MgCl_2$, 0.1% NP40, and protease inhibitors Complete, Roche]. Protein content was estimated by BCA (Pierce, Rockford, IL). Proteasomal activity was measured as described previously (10). One hundred nanograms of purified proteasomes (13) were exposed to proteasome inhibitors and activity was determined with 100 μmol/L fluorogenic substrate [succinyl-Leu-Leu-Val-Tyr-7-amido-4-methylcoumarin (suc-LLVY-AMC), Bachem, Weil am Rhein, Germany]. The calpain activity was measured in cell lysates using the calpain substrate suc-LY-AMC (Calbiochem) as described (14) and verified by the specific calpain inhibitor III (Calbiochem).

Cell cycle analysis by flow cytometry. For cell cycle analysis, cells were treated for 24 or 48 hours with BSc2118 (0-1,000 nmol/L). After the incubation period, melanoma cells were fixed in ice-cold 70% ethanol in PBS and stored at −20°C. After washing, cells were resuspended in PBS containing 200 μg DNase-free RNase A (Sigma) for 20 minutes at room temperature. Propidium iodide (Sigma) was added to a final concentration of 5 μg/mL and cells were stained for at least 2 hours at 4°C. Analysis was done on a FACSCalibur flow cytometer (Becton Dickinson, San Diego, CA) and analyzed by CellQuest software.

Apoptosis measurement using flow cytometry. Apoptosis was analyzed after 24 and 48 hours of exposure of melanoma cells to BSc2118 (10-500 nmol/L), PD150606 (25-300 μmol/L), or BAY 11-7082 (5-10 μmol/L). Apoptotic cells were labeled by Annexin V–FITC, necrotic cells were marked by the uptake of propidium iodide according to the instructions from the manufacturer (BioSource, Camarillo, CA). Living cells are defined as negative for both Annexin V and propidium iodide, early apoptotic cells are positive for Annexin V only, and late apoptotic and necrotic cells are positive for both dyes (15, 16). The samples were analyzed on a FACSCalibur flow cytometer (Becton Dickinson) and evaluated using CellQuest software.

Immunoblot analysis. Protein expression in melanoma cells was analyzed as shown before (17). Briefly, samples containing 50 μg of protein were separated on a 10% SDS-PAGE, transferred to nitrocellulose membranes, and probed with rabbit polyclonal anti-IκBα antibody and mouse anti-β-tubulin antibody (Santa Cruz Biotechnology, Santa Cruz, CA).

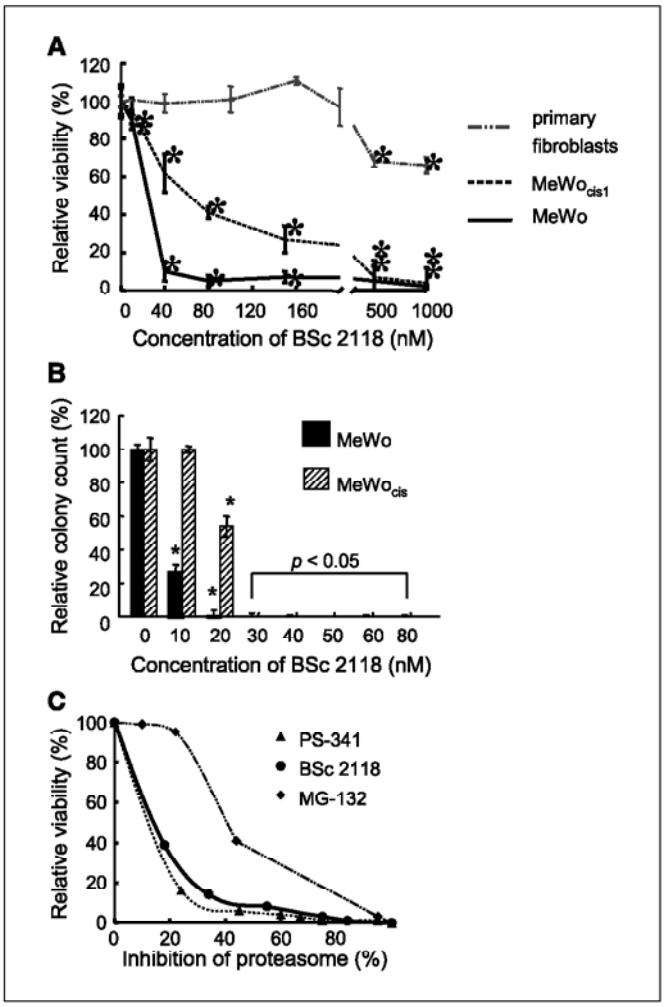

Figure 1. The effects of proteasome inhibitors on viability of melanoma cells and primary human fibroblasts *in vitro*. *A*, cisplatin-sensitive melanoma cells (MeWo), cisplatin-resistant melanoma cells ($MeWo_{cis1}$), and primary human fibroblasts were treated with BSc2118 at final concentrations ranging from 0 to 1,000 nmol/L for 48 hours, and relative viability was displayed as percentage of control group. *B*, the effect of proteasome inhibitor BSc2118 on colony formation. MeWo and $MeWo_{cis1}$ cells were treated with BSc2118 at final concentrations ranging from 0 to 80 nmol/L in quadruplicate for 15 days. Colony count (*columns*) in untreated groups was defined as 100%; *bars*, SD. *, $P < 0.05$ compared with the control group (Student's *t* test). *C*, viability of MeWo cells after 48-hour exposure to proteasome inhibitor MG-132, BSc2118, or PS-341 (0-1,000 nmol/L), dependent on inhibition of purified 20S proteasome by each particular inhibitor, respectively.

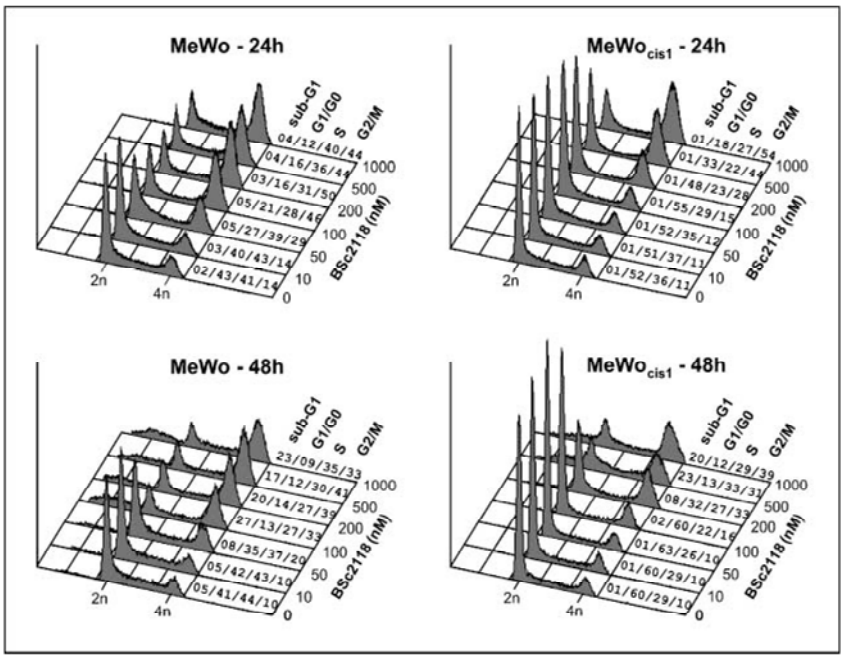

Figure 2. Cell cycle analysis in melanoma cells after BSc2118 treatment. MeWo and MeWo$_{cis1}$ cells were treated with BSc2118 (0-1,000 nmol/L) for 24 hours (*top*) and 48 hours (*bottom*). The cell cycle profile of propidium iodide–stained cells was determined by fluorescence-activated cell sorting analysis. *Numbers beneath each histogram,* percentages of cells in apoptosis (sub-G_1 peak), in phase G_1-G_0, phase S, and phase G_2-M of the cell cycle, respectively. *Z-axis,* concentrations of BSc2118. In MeWo cells, cell cycle arrest is already induced at low BSc2118 concentrations. In MeWo$_{cis1}$ cells, cell cycle arrest requires higher BSc2118 concentrations.

The immunoblots were visualized with horseradish peroxidase–conjugated secondary antibodies (Jackson Immunoresearch, Cambridgeshire, United Kingdom) and enhanced by chemiluminescence (Roche).

Electrophoretic mobility shift assay. TNF-induced nuclear binding of NF-κB was done by electrophoretic mobility shift assay (EMSA) in nuclear extracts of melanoma cells. Nuclear extracts were prepared using a modified nonionic detergent method as described before (18). For detection of NF-κB in nuclear extracts, specific oligonucleotides (5′-GATCCAGGGCTGGGGATTCCCCATCTCCACAGG-3′; 5′-GATCCCTGTGGAGATGGGGAATCCCCAGCCCTG-3′) from the H-2K region of the MHC-I promoter were labeled with [α^{32}P]ATP in the presence of 500 mmol/L deoxynucleotide triphosphates without ATP for 30 minutes at 37°C and for 5 minutes at 65°C. Nonincorporated radioactivity was removed by NICK Sephadex G-50 columns (Amersham Biosciences, Uppsala, Sweden). For the binding reaction, 5 μg of nuclear extracts were incubated with 2-fold shift buffer [40 mmol/L HEPES (pH 7.9), 120 mmol/L KCl, 8% Ficoll], 0.5 μg/μL bovine serum albumin, 5 mmol/L DTT, 0.5 μg/μL poly(deoxyinosinic-deoxycytidylic acid), and 20,000 cpm of labeled H2-K oligo for 30 minutes at 30°C. DNA binding was analyzed on 5% polyacrylamide gels by autoradiography.

Statistical analysis. Data of cell viability and protease activity experiments were presented as means ± SD and Student's t test (two-tailed) was used to compare differences between analyzed groups. The statistical analysis for flow cytometry results was done using two-sided χ^2 test.

Results

Cytotoxic and cytostatic effects of proteasome inhibition on human melanoma cells. To determine the cytotoxic and cytostatic effects of proteasome inhibition on human melanoma cells, MeWo or MeWo$_{cis1}$ cells were exposed to different concentrations of proteasome inhibitor BSc2118 for 48 hours (Fig. 1*A*) and the viability of the cells was determined by crystal violet assay. Exposure of MeWo and MeWo$_{cis1}$ cells to the proteasome inhibitor resulted in a dose-dependent reduction of cell viability. The IC_{50} for BSc2118 determined was 30 nmol/L for MeWo cells and 70 nmol/L for MeWo$_{cis1}$ cells (Fig. 1*A*). Thus, although both melanoma cell lines are sensitive to BSc2118, considerably larger amounts of the inhibitor are required to induce a reduction of cell viability in MeWo$_{cis1}$ cells. For further control, we assessed the cytotoxic effect of BSc2118 on nonmalignant primary human fibroblasts (Fig. 1*A*). In contrast to melanoma cells, primary human fibroblasts were strikingly insensitive to proteasome inhibition and extremely high BSc2118 concentrations (>500 nmol/L) were required to affect their viability.

To investigate the effect of proteasome inhibition on tumor cell outgrowth, we did cell colony formation assay. MeWo and MeWo$_{cis1}$ cells were exposed to serial concentrations of BSc2118 for 15 days and colonies formed were counted. As revealed in Fig. 1*B*, <10 nmol/L of BSc2118 were needed to achieve a 50% reduction in outgrowth of MeWo cells. An inhibitor concentration of 20 nmol/L was sufficient to stop MeWo cell colony formation completely. In contrast, MeWo$_{cis1}$ cells turned out to be considerably more resistant to proteasome inhibition. Nevertheless, a BSc2118 concentration of 30 nmol/L was sufficient to completely impair colony formation.

To test the potency and selectivity of BSc2118, we compared its antiproliferative effect on melanoma cells with that of the commonly used proteasome inhibitor MG-132, which displays structural similarity to BSc2118, and the inhibitor PS-341, which was recently approved for clinical application in relapsed multiple myeloma (19, 20). For this purpose, melanoma cells were incubated with increasing inhibitor concentrations (0-1,000 nmol/L) and cell viability was related to the degree of proteasome inhibition. This method permits correlation of proteasome inhibitors with different K_i values (BSc2118, 45 nmol/L; PS-341, 0.6 nmol/L; MG-132, 20 nmol/L) and to compare their antiproliferative efficiency on malignant cells (21). Correlating the reduction in cell viability with the ability to inhibit proteasome activity revealed that BSc2118 is considerably more efficient in affecting cell viability than MG-132. Furthermore, BSc2118 exhibited a similar antiproliferative effect as PS-341 (Fig. 1*C*). Together, these data show that inhibition of proteasome activity is able to effectively reduce the viability of MeWo and MeWo$_{cis1}$ cells at low concentrations that are not toxic to primary human fibroblasts.

MeWo$_{cis1}$ cells require higher inhibitor concentrations for cell cycle arrest. Because proteasome inhibitors are known to affect cell cycle progression, we next analyzed the effect of BSc2118 on the cell cycle in MeWo and MeWo$_{cis1}$ cells. Flow cytometry–based cell cycle analysis revealed a BSc2118-triggered G_2-M arrest in cisplatin-sensitive and cisplatin-resistant melanoma cells (Fig. 2). The presence of a sub-G_1 peak that indirectly indicates apoptotic cell death (22) is detectable mainly after 48 hours of inhibitor treatment (Fig. 2). A similar effect was also observed when inhibitor-treated cells were analyzed by Annexin V staining (data not shown). Bromodeoxyuridine (BrdUrd) incorporation experiments also revealed an effect of proteasome inhibition on cell cycle progression in the G_1-S phase in that both cell lines stopped to incorporate BrdUrd after 48 hours (Supplementary Fig. S1). As observed in the experiments above (Fig. 1), MeWo$_{cis1}$ cells were again considerably more resistant against proteasome inhibition than MeWo cells.

Proteasomes of both MeWo and MeWo$_{cis1}$ cells are equally sensitive to BSc2118. One important observation of the experiments done thus far is that both MeWo and MeWo$_{cis1}$ cells react similarly to proteasome inhibition. However, significantly higher inhibitor concentration had to be applied to MeWo$_{cis1}$ cells to obtain the same effects as in MeWo cells. Because it had been reported that proteasomes can become resistant to inhibitors (23), our data raised the possibility that proteasomes of MeWo$_{cis1}$ cells may exhibit a reduced susceptibility toward proteasome inhibitors.

Therefore, we directly assessed the inhibitory effect of BSc2118 on cellular proteasome activity by exposing both MeWo and MeWo$_{cis1}$ cells to different concentrations of BSc2118 and by measuring the chymotrypsin-like proteasome activity in cell lysates using the fluorogenic peptide substrate suc-LLVY-AMC. As shown in Fig. 3, reduction of the chymotrypsin-like proteasome activity by BSc2118 at two time points (1 and 4 hours), and at all inhibitor concentrations used, was almost identical in both cisplatin-sensitive and cisplatin-insensitive melanoma cells (Fig. 3*A* and *B*). These experiments confirm that BSc2118 penetrates both cell lines with the same efficiency, and, more importantly, that proteasomes of MeWo and MeWo$_{cis1}$ cells are equally sensitive to BSc2118.

We also tested MeWo$_{cis1}$ cells with respect to multidrug resistance by investigating activity of the multidrug resistance–associated protein (MRP1). However, no enhanced MRP-1 activity could be determined as defined by calcein-AM assay (data not shown). From these experiments, we therefore conclude that the relative resistance of MeWo$_{cis1}$ cells toward proteasome inhibition is not caused by the different effect of proteasome inhibitors on MeWo and MeWo$_{cis1}$ cells, but that the observed resistance is more likely the consequence of altered postproteasomal or proteasome-independent mechanisms.

IκBα degradation and NF-κB activation in MeWo$_{cis1}$ cells is proteasome independent. To study a potential proteasome-independent mechanism of resistance in melanoma cells at the molecular level, we focused on the IκBα expression as an indicator for NF-κB activation. In this context, it has been shown that IκBα is mainly degraded in a proteasome-dependent manner, but that in some cells and under certain physiologic conditions IκBα degradation can also occur independently of the proteasome (24). Because it is established that NF-κB can interfere with the induction of cell death, and based on the results obtained above, we hypothesized that the increased resistance of MeWo$_{cis1}$ cells to proteasome inhibition may be due to an enhanced constitutive NF-κB activation as it has been described for other tumor cells (25, 26). In the canonical NF-κB activation pathway, TNF stimulates the phosphorylation and proteasome-dependent degradation of IκBα. This process results in the release and transfer of NF-κB into the nucleus. Because the activation of NF-κB in the cytosol requires proteasome activity, the inhibition of proteasome-dependent IκBα degradation by proteasome inhibitors should also impair NF-κB activation (27).

At first, we analyzed IκBα expression in both cell lines after stimulation of the cells with TNF, and in the absence or presence of BSc2118. In comparison to MeWo cells, longer TNF stimulation of MeWo$_{cis1}$ cells was required to induce degradation of IκBα (data not shown). As expected, TNF-induced IκBα degradation was stabilized by proteasome inhibition in parental MeWo cells (Fig. 4*A*, *top*). However, in complete contrast, proteasome inhibition by BSc2118 did not result in the expected stabilization of IκBα in MeWo$_{cis1}$ cells (Fig. 4*A*, *bottom*), suggesting that the NF-κB pathway is defective or might have been altered in MeWo$_{cis1}$ cells.

To assess nuclear NF-κB translocation, EMSAs were done. As expected from the data shown above, activation of NF-κB was impaired by proteasome inhibition in MeWo cells (Fig. 4*B*). In contrast, and in complete accordance with the results shown in Fig. 4*A*, inhibition of proteasomes in MeWo$_{cis1}$ cells did not prevent nuclear translocation of NF-κB. The low NF-κB baseline binding observed in both cell lines (also see Fig. 6*A*) excludes the above

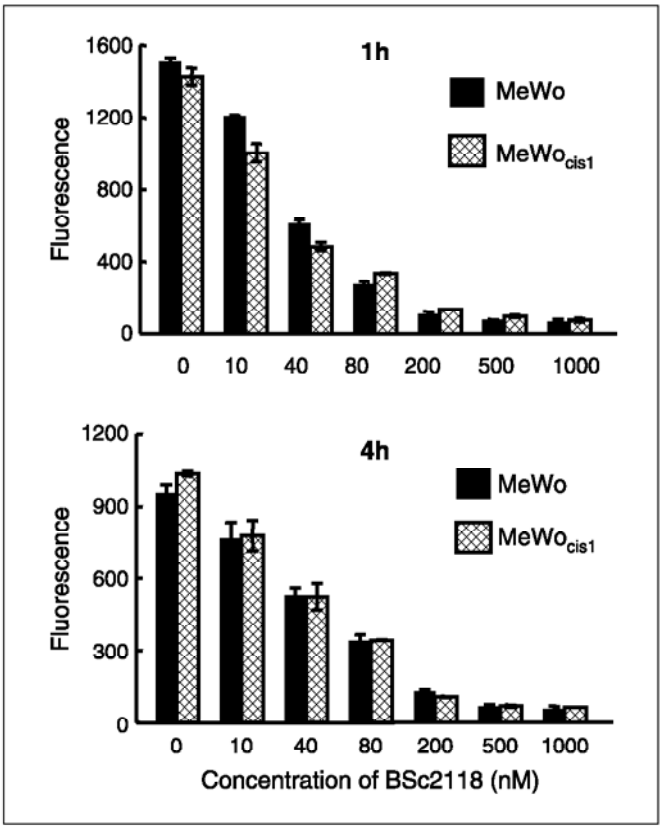

Figure 3. Peptide-hydrolyzing activity of 20S proteasome in lysates from MeWo and MeWo$_{cis1}$ cells. The proteolytic activity was measured after 1 hour (*top*) and 4 hours (*bottom*) of incubation with proteasome inhibitor BSc2118 (0-1,000 nmol/L). *Columns*, mean fluorescence of released AMC (*columns*) from the proteasome substrate suc-LLVY-AMC, normalized to 1 mg protein per milliliter of cell lysate; *bars*, SD.

hypothesis that high constitutive NF-κB activity is responsible for the observed effects in $MeWo_{cis1}$ cells. Together, however, these data also indicate the existence of an imbalance in the NF-κB signaling pathway in $MeWo_{cis1}$ cells and suggest that IκBα degradation, and hence NF-κB activation, might be controlled by a proteasome-independent mechanism.

Role for calpain in IκBα degradation in $MeWo_{cis1}$ cells. Although IκBα degradation is attributed primarily to the ubiquitin-proteasome pathway (28), it has also been shown that alternative other proteases, i.e., calpain, are involved in the regulation of IκBα stability (8). To investigate whether calpain might be responsible for the observed TNF-induced IκBα degradation in $MeWo_{cis1}$ cells, the calpain-specific inhibitor PD150606 was used (29). PD150606 binds to the noncatalytic site of activated calpain when the substrate is bound to the protease (29) and importantly does not inhibit proteasome activity. To this end, melanoma cells were preincubated with BSc2118, MG-132, or PD150606 for 1 hour, followed by TNF stimulation for 20 minutes for MeWo cells and 40 minutes for $MeWo_{cis1}$ cells. As a control and to confirm IκBα degradation, these melanoma cells were exposed to TNF alone. As shown in Fig. 5*A* (*top*), TNF-induced IκBα degradation was prevented in the parental MeWo cell line by proteasome inhibitors BSc2118 and MG-132. Interestingly, inhibition of calpain also was able to confer IκBα stability, indicating that in MeWo cells two parallel pathways for NF-κB activation coexist. In contrast, although the proteasome inhibitors failed to confer IκBα stability in $MeWo_{cis1}$ cells, only the exposure of $MeWo_{cis1}$ cells to calpain inhibitor abolished TNF-induced degradation of IκBα (Fig. 5*A*, *bottom*) and this effect was dose dependent (Fig. 5*B*). Similar results were obtained using different calpain inhibitors, such as E64 (data not shown).

In addition, comparison of cellular calpain- and proteasome-specific proteolytic activities in both cell lines revealed different biological effects; whereas both melanoma cell lines exhibited similar proteasome activity, calpain activity was significantly up-regulated in $MeWo_{cis1}$ cells (Fig. 5*C*), suggesting a shift toward an increased use of the calpain-dependent proteolytic pathway in $MeWo_{cis1}$ cells.

Inhibition of calpain prevents NF-κB activation in cisplatin-resistant human melanoma cells. To address the question whether stabilization of IκBα by calpain inhibition also accompanies impeded NF-κB nuclear translocation in $MeWo_{cis1}$ cells, EMSA assays were done. In agreement with the data shown above,

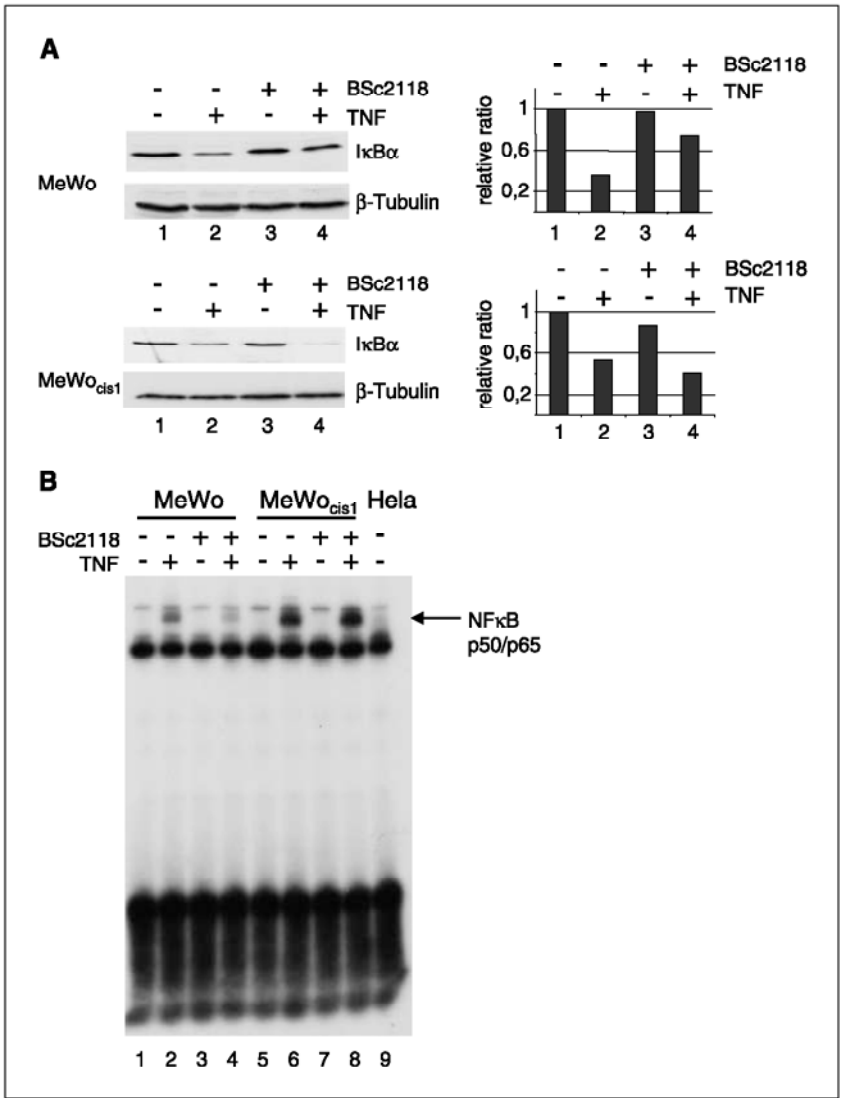

Figure 4. IκBα and NF-κB expression in MeWo and $MeWo_{cis1}$ cells. *A*, IκBα detection in lysates from MeWo cells (*top*) and $MeWo_{cis1}$ cells (*bottom*) by immunoblotting. Cells were treated as follows: *lane 1*, nontreated cells; *lane 2*, TNF for up to 1 hour; *lane 3*, 1 μmol/L BSc2118 for 1 hour; *lane 4*, 1 μmol/L BSc2118 for 1 hour followed by TNF 2,000 units/mL for up to 1 hour. In MeWo cells, BSc2118 inhibited TNF-induced IκBα degradation. In contrast, in $MeWo_{cis1}$ cells, IκBα was degraded in the presence of BSc2118. β-Tubulin was used as a loading control. Diagrams display densitometric analysis of IκBα immunoblots. *B*, EMSAs were applied to evaluate NF-κB activation induced by 2,000 units/mL TNF in MeWo and $MeWo_{cis1}$ cells in the presence and absence of proteasome inhibitor BSc2118. MeWo and $MeWo_{cis1}$ cells were preincubated with 1 μmol/L inhibitor BSc2118 for 1 hour, followed by TNF incubation for 20 and 40 minutes, respectively. In MeWo cells (*lanes 1-4*), BSc2118 reduced the TNF-induced NF-κB activation. In $MeWo_{cis1}$ cells (*lanes 5-8*), NF-κB was still activated in the presence of BSc2118. NF-κB detection in nuclear extracts from nonstimulated HeLa cells is shown as a control (*lane 9*).

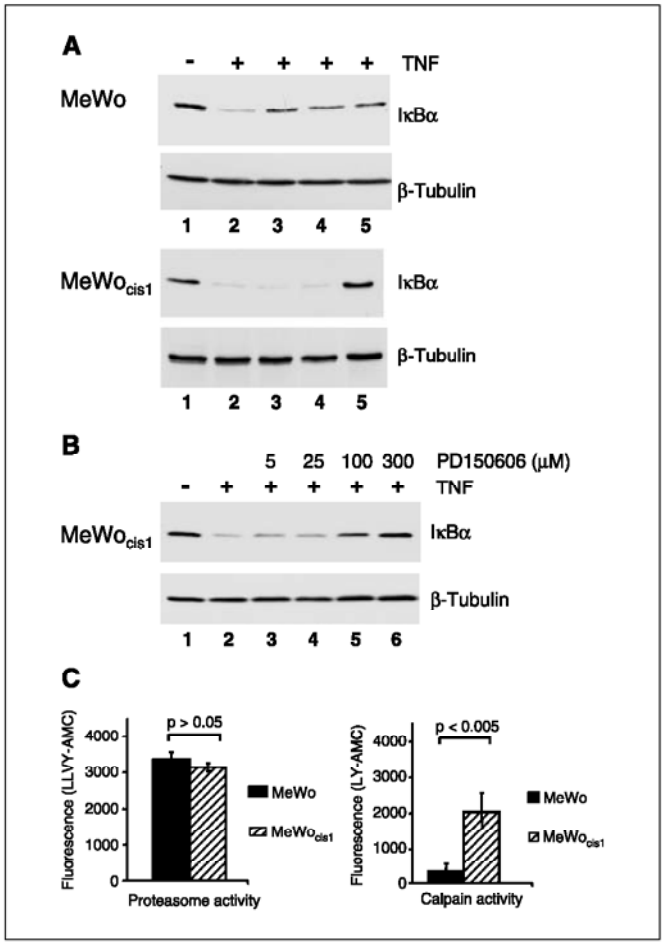

Figure 5. Effects of proteasome and/or calpain inhibition on IκBα expression and measurement of proteasome and calpain activity in human melanoma cells. *A*, immunoblot analysis of IκBα in MeWo cells (*top*) and in $MeWo_{cis1}$ cells (*bottom*). Lanes are described as follows: *lane 1*, control cells; *lane 2*, incubation with TNF 2,000 units/mL; *lane 3*, preincubation with 1 μmol/L BSc2118 followed by TNF 2,000 units/mL; *lane 4*, preincubation with 1 μmol/L MG-132 followed by TNF 2,000 units/mL; *lane 5*, preincubation with 300 μmol/L calpain inhibitor PD-150606 followed by TNF 2,000 units/mL. In MeWo cells, both proteasome and calpain inhibitors stabilize IκBα signal (*top, lanes 3-5*), whereas in $MeWo_{cis1}$ cells only incubation with calpain inhibitor inhibits TNF-induced IκBα degradation. *B*, immunoblot analysis of IκBα in $MeWo_{cis1}$ cells pretreated for 1 hour with increasing concentrations of PD150606 (5-300 μmol/L, *lanes 3-6*) followed by TNF 2,000 units/mL stimulation revealed dose-dependent stabilization of IκBα signal. *C*, calpain activity is enhanced in $MeWo_{cis1}$ cells compared with MeWo cells. *Left*, proteasome activity in lysates from MeWo and $MeWo_{cis1}$ cells was normalized to protein content and displayed as mean fluorescence of released AMC. The proteasome activity is similar for both cell lines. *Right*, calpain activity in lysates derived from MeWo and $MeWo_{cis1}$ cells was normalized to protein content. *Columns*, calpain activity estimated as the difference between total fluorescence of calpain substrate suc-LY-AMC in reaction buffer without inhibitors and the remaining fluorescence in presence of 50 μmol/L calpain inhibitor III. In $MeWo_{cis1}$ cells, calpain activity is six times higher than in MeWo cells; *bars*, SD.

inhibition of calpain activity in $MeWo_{cis1}$ cells completely abolished TNF-induced NF-κB activation (Fig. 6*A*, *right*). In contrast, no significant effect was observed on MeWo cells whose NF-κB activation system is Bsc2118 sensitive (Fig. 6*A*, *left*).

To study a possible effect of calpain inhibition with PD150606 and the concomitant inhibition of NF-κB activation in $MeWo_{cis1}$ cells, we examined the induction of apoptosis. Annexin V staining revealed a correlation with increasing calpain inhibitor concentrations and an increase in the relative amount of apoptotic $MeWo_{cis1}$ cells. In contrast, the relative amount of Annexin V–positive MeWo cells remained almost unchanged (Fig. 6*B*, *a-c*, *bottom right quadrant*). In fact, considerably more MeWo cells underwent necrosis as evidenced by double-positive staining for propidium iodide and Annexin V. However, the relative number of $MeWo_{cis1}$ necrotic cells remained constant when the cells were treated with the calpain inhibitor (Fig. 6*B*, *a-c*, *top right quadrant*). Interestingly, the inhibitor of TNF-induced proteasome-dependent IκBα degradation, BAY 11-7082, induced more cell death in MeWo cells than in the $MeWo_{cis1}$ cells (Fig. 6*B*, *d*, *top* and *bottom right quadrants*).

These experiments show that in a concentration-dependent manner, calpain inhibition can affect cell viability of cisplatin-resistant cells. However, given the lack of a precise molecular mechanism, the observed effect on apoptosis of chemoresistant cells may only be a correlative one.

Additive effects of proteasome and calpain inhibition on cell viability. If the increased resistance of $MeWo_{cis1}$ cells to proteasome inhibitor is caused by a shift to calpain-mediated IκBα degradation, treatment of melanoma cells with calpain inhibitor should also affect the viability of the cells. To address this question, we analyzed the effects of BSc2118 and/or calpain inhibitor PD150606 on the viability of MeWo and $MeWo_{cis1}$ cells. Calpain inhibitor treatment at 25 μmol/L by itself affected cell viability in both cell lines only marginally (Fig. 6*C*). As shown before, BSc2118 alone reduced cell viability by ~60%. However, although the combination of both inhibitors resulted only in a slight additional reduction of MeWo cell viability, combined inhibitor treatment of $MeWo_{cis1}$ cells had a significantly stronger effect and reduced cell viability to ~10% (Fig. 6*C*). It is of note that addition of cisplatin to proteasome/calpain inhibitor–treated $MeWo_{cis1}$ cells did not affect cell viability stronger than both inhibitors alone (Supplementary Fig. S2).

Thus, our data show that the combined treatment of $MeWo_{cis1}$ cells with BSc2118 and PD150606 affects two different proteolytic pathways and can enhance the proteasome inhibitor–mediated death of the tumor cells, especially of the cisplatin-resistant cells.

Discussion

Cisplatin resistance, or more generally chemotherapy resistance, is a major obstacle in the treatment of metastatic melanoma and other solid tumors. However, in most cases, severe toxicity precludes the administration of higher doses of chemotherapeutic agents. One of the practical ways to solve this problem in the clinic is to combine traditional chemotherapeutics with their synergistic modulators, thus improving therapeutic efficacy without increasing toxicity. Moreover, analysis of mechanisms leading to chemotherapy resistance might result in the identification of targets that will safely and effectively enhance therapeutic success. In this context, inhibition of the proteasome represents a new target for cancer therapy (30).

In this study, we first analyzed the effects of the new proteasome inhibitor BSc2118 on both cisplatin-resistant and cisplatin-sensitive melanoma cells. We found that BSc2118 induced reduction in cell viability in both MeWo and $MeWo_{cis1}$ cell lines, diminished colony formation, promoted G_2-M cell cycle arrest, and apoptosis. However, the cisplatin-resistant cells required considerably higher inhibitor concentrations to exert the same biological effects as seen in the parental cisplatin-sensitive cells. Nevertheless, the extent of proteasome inhibition was identical in both cell lines, suggesting the existence of proteasome-independent mechanisms for the relative proteasome inhibitor resistance in $MeWo_{cis1}$ cells.

In WEHI-231 B cells, it has been shown that prolonged NF-κB activation is associated with continued degradation of IκBα and that the NF-κB pathway may participate in proteasome inhibitor resistance (24). On the other hand, Hideshima et al. (31) showed that NF-κB blockade by proteasome inhibition cannot account for all of the antitumor activity observed in multiple myeloma. Interestingly, our analysis of the NF-κB pathway in $MeWo_{cis1}$ melanoma cells revealed a proteasome-independent but calpain inhibitor–mediated IκBα stabilization and inhibition of NF-κB activation. In neuronal cells, it was shown previously that binding of glutamate to its receptor induces a shift from a proteasome-dependent to a calpain-dependent IκBα degradation followed by NF-κB activation and that calpain-dependent IκBα degradation plays a role in inflammation, as well as in neuronal cell survival and cell death (32). Interestingly, in MeWo cells, both the proteasome and the calpain-sensitive IκBα degradation seem to coexist, whereas in $MeWo_{cis1}$ cells the calpain-sensitive IκBα degradation predominates. Furthermore, calpain activity in lysates of $MeWo_{cis1}$ cells was strongly increased, suggesting for the first time that calpain may play a role in chemotherapy resistance in melanoma cells. Thus far, it has been acknowledged that calpain activity can lead tumor cells to apoptosis (33) and is involved in genistein-induced or cisplatin-mediated apoptosis (5, 34). In HCT 116 human colon carcinoma cells, it was shown that cisplatin induced

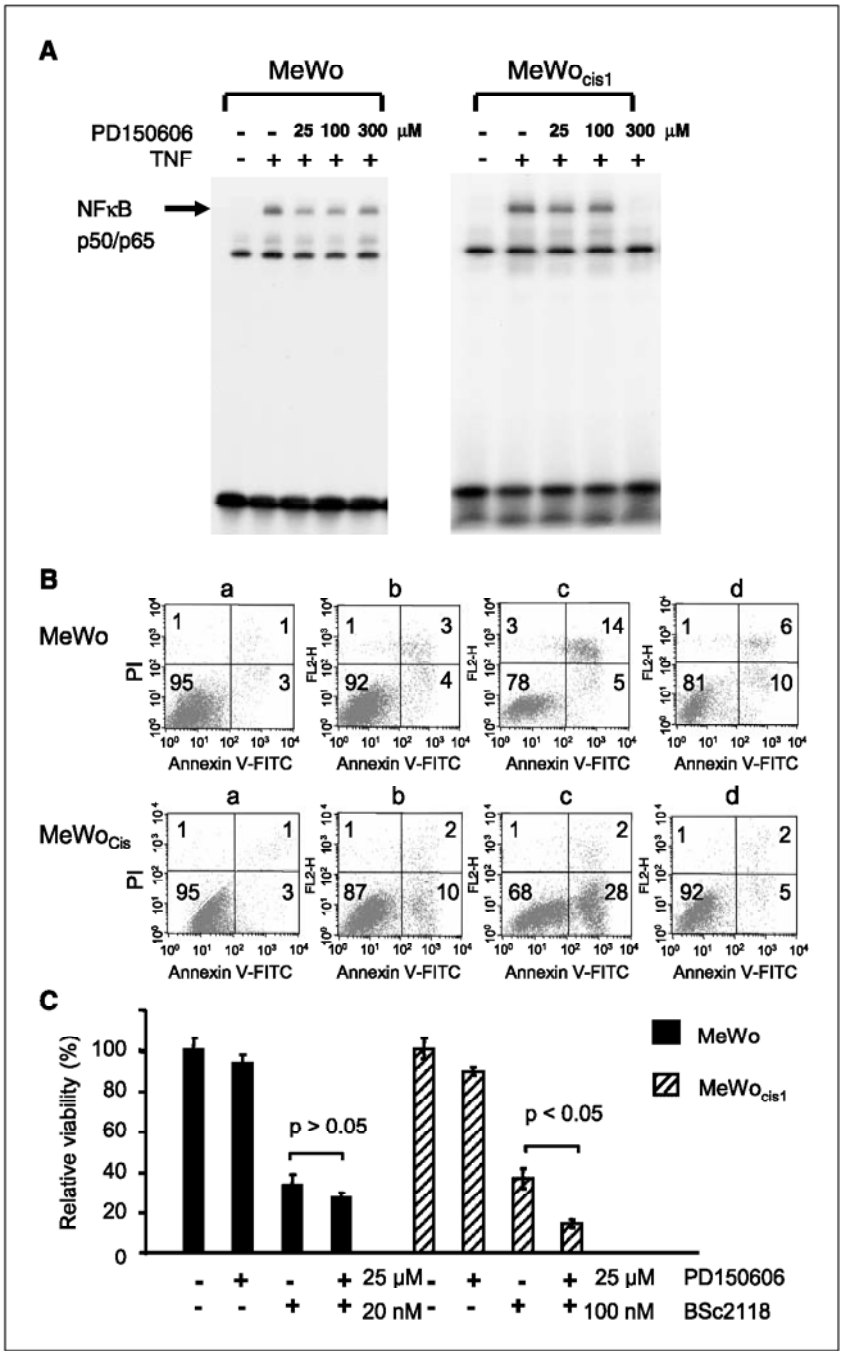

Figure 6. NF-κB expression, apoptosis, and viability analysis in MeWo and $MeWo_{cis1}$ cells after calpain inhibition. *A*, EMSA was used to evaluate NF-κB nuclear translocation induced by 2,000 units/mL TNF in MeWo and $MeWo_{cis1}$ cells in the absence or presence of PD150606 (25-300 μmol/L). In $MeWo_{cis1}$ cells, PD150606 at 300 μmol/L completely blocked TNF-induced NF-κB activation (*right*), whereas in MeWo cells no stabilization of the NF-κB signal was observed (*left*). *B*, apoptosis analysis of MeWo (*top*) and $MeWo_{cis1}$ cells (*bottom*) either nontreated (*a*) or after 48-hour exposure to PD150606 at 100 μmol/L (*b*) or 300 μmol/L PD150606 (*c*), or after 48 hours exposure to BAY 11-7082 10 μmol/L (*d*). Cells were stained with Annexin V (*X axis*) and propidium iodide (*PI, Y axis*) and analyzed by flow cytometry. Intact cells are negative for both dyes (*bottom left quadrant*), early apoptotic cells are positive for Annexin V (*bottom right quadrant*), late apoptotic or necrotic cells are positive for Annexin V and propidium iodide (*top right quadrant*), necrotic cells are positive for propidium iodide only (*top left quadrant*). *Numbers in quadrants*, percentages of stained cells. All groups are different from each control at χ^2 test ($P < 0.05$). In $MeWo_{cis1}$ cells, the fraction of early apoptotic cells is increased at 100 and 300 μmol/L PD150606, whereas in MeWo cells PD150606 induced necrosis. Treatment with BAY 11-7082 induced cell death in MeWo cells but not in $MeWo_{cis1}$ cells. *C*, effect of proteasome and calpain inhibitors on the viability of MeWo and $MeWo_{cis1}$ cells. Cells were incubated with 25 μmol/L PD150606 and/or BSc2118 for 72 hours and cell viability was estimated with crystal violet assays. For BSc2118 incubated groups 20 nmol/L was required for MeWo cells versus 100 nmol/L for $MeWo_{cis1}$ cells to achieve comparable percentages of cell viability reduction. The strongest cytotoxic/cytostatic effect was observed after combined treatment with PD150606 and BSc2118 in $MeWo_{cis1}$ cells.

increased cytosolic calcium level, calpain activation, as well as endoplasmic reticulum stress (5). Interestingly, the cisplatin-resistant $MeWo_{cis1}$ cells studied here exhibit increased calpain activity even in the absence of cisplatin and already the inhibition of calpain activity is able to induce apoptosis. This latter result may be explained in part by the recently described apoptotic defects in $MeWo_{cis1}$ cells (11) and by a shift in the NF-κB signaling pathway toward an ubiquitin-proteasome system independent IκBα degradation. Calpain- and proteasome-dependent NF-κB activation following TNF treatment has also been observed in human HepG2 cells (8). When ubiquitinating enzymes were inactivated, IκBα proteolysis occurred only in a strictly calpain-dependent manner (8). However, it is not currently defined which steps in the signaling cascade are affected in the $MeWo_{cis}$ cells that result in an almost complete shift toward TNF-induced, calpain-sensitive IκBα degradation. In this context, it is important to note that it has recently been shown that bortezomib and cisplatin induce apoptosis via endoplasmic reticulum stress in pancreatic cancer cells. Therefore, selecting cisplatin-resistant cells could have resulted in selection of endoplasmic reticulum stress–resistant cells and thus may in part account for the observed differences in growth arrest and apoptosis induction between MeWo and $MeWo_{cis}$ cell lines (35).

Our experiments also show that the combined inhibition of both the proteasome and calpain affects the viability of $MeWo_{cis1}$ cells considerably more than when each agent is applied alone, resulting in an almost complete cell death of $MeWo_{cis1}$ cells. It is interesting to note that inhibition of calpain with nontoxic concentrations of PD150606 alone had no significant effect on cell viability of either MeWo or $MeWo_{cis1}$ cells and that only the application of PD150606 together with BSc2118 significantly increased the antitumor activity of proteasome inhibition on cisplatin-resistant cells. Thus, by combining proteasome and calpain inhibitors, our data may display new therapeutic strategies for the treatment of chemotherapy-resistant melanoma cells.

Acknowledgments

Received 7/25/2005; revised 5/3/2006; accepted 5/26/2006.

Grant support: European Molecular Biology Organization grant ASTF 94.00-04 (I. Młynarczuk-Biały).

The costs of publication of this article were defrayed in part by the payment of page charges. This article must therefore be hereby marked *advertisement* in accordance with 18 U.S.C. Section 1734 solely to indicate this fact.

We thank Ingrid Krenz and Iris Gruska for expert technical assistance and Naomi Weizenbaum for correcting the manuscript.

References

1. Slominski A, Wortsman J, Carlson AJ, Matsuoka LY, Balch CM, Mihm MC. Malignant melanoma. Arch Pathol Lab Med 2001;125:1295–306.
2. Chung ES, Sabel MS, Sondak VK. Current state of treatment for primary cutaneous melanoma. Clin Exp Med 2004;4:65–77.
3. Reedijk J. New clues for platinum antitumor chemistry: kinetically controlled metal binding to DNA. Proc Natl Acad Sci U S A 2003;100:3611–6.
4. Rockmann H, Schadendorf D. Drug resistance in human melanoma: mechanisms and therapeutic opportunities. Onkologie 2003;26:581–7.
5. Mandic A, Hansson J, Linder S, Shoshan MC. Cisplatin induces endoplasmic reticulum stress and nucleus-independent apoptotic signaling. J Biol Chem 2003;278:9100–6.
6. Bunn PA, Jr. The potential role of proteasome inhibitors in the treatment of lung cancer. Clin Cancer Res 2004;10:4263–5s.
7. Bold RJ, Virudachalam S, McConkey DJ. Chemosensitization of pancreatic cancer by inhibition of the 26S proteasome. J Surg Res 2001;100:11–7.
8. Han Y, Weinman S, Boldogh I, Walker RK, Brasier AR. Tumor necrosis factor-α-inducible IκBα proteolysis mediated by cytosolic m-calpain. A mechanism parallel to the ubiquitin-proteasome pathway for nuclear factor-κB activation. J Biol Chem 1999;274:787–94.
9. Goll DE, Thompson VF, Li H, Wei W, Cong J. The calpain system. Physiol Rev 2003;83:731–801.
10. Braun HA, Umbreen S, Groll M, et al. Tripeptide mimetics inhibit the 20S proteasome by covalent bonding to the active threonines. J Biol Chem 2005;280:28394–401.
11. Helmbach H, Kern MA, Rossmann E, et al. Drug resistance towards etoposide and cisplatin in human melanoma cells is associated with drug-dependent apoptosis deficiency. J Invest Dermatol 2002;118:923–32.
12. Mickuviene I, Kirveliene V, Juodka B. Experimental survey of non-clonogenic viability assays for adherent cells *in vitro*. Toxicol In Vitro 2004;18:639–48.
13. Groettrup M, Ruppert T, Kuehn L, et al. The interferon-γ-inducible 11S regulator (PA28) and the LMP2/LMP7 subunits govern the peptide production by the 20S proteasome *in vitro*. J Biol Chem 1995;270:23808–15.
14. Edelstein CL, Wieder ED, Yaqoob MM, et al. The role of cysteine proteases in hypoxia-induced rat renal proximal tubular injury. Proc Natl Acad Sci U S A 1995;92:7662–6.
15. Homburg CH, de Haas M, von dem Borne AE, Verhoeven AJ, Reutelingsperger CP, Roos D. Human neutrophils lose their surface FcγRIII and acquire Annexin V binding sites during apoptosis *in vitro*. Blood 1995;85:532–40.
16. Boersma AW, Nooter K, Burger H, Kortland CJ, Stoter G. Bax upregulation is an early event in cisplatin-induced apoptosis in human testicular germ-cell tumor cell line NT2, as quantitated by flow cytometry. Cytometry 1997;27:275–82.
17. Sun Y, Sijts AJ, Song M, et al. Expression of the proteasome activator PA28 rescues the presentation of a cytotoxic T lymphocyte epitope on melanoma cells. Cancer Res 2002;62:2875–82.
18. Dignam JD, Lebovitz RM, Roeder RG. Accurate transcription initiation by RNA polymerase II in a soluble extract from isolated mammalian nuclei. Nucleic Acids Res 1983;11:1475–89.
19. Richardson PG, Barlogie B, Berenson J, et al. A phase 2 study of bortezomib in relapsed, refractory myeloma. N Engl J Med 2003;348:2609–17.
20. Jagannath S, Barlogie B, Berenson J, et al. A phase 2 study of two doses of bortezomib in relapsed or refractory myeloma. Br J Haematol 2004;127:165–72.
21. Adams J, Palombella VJ, Sausville EA, et al. Proteasome inhibitors: a novel class of potent and effective antitumor agents. Cancer Res 1999;59:2615–22.
22. Schmid I, Uittenbogaart CH, Giorgi JV. Sensitive method for measuring apoptosis and cell surface phenotype in human thymocytes by flow cytometry. Cytometry 1994;15:12–20.
23. Glas R, Bogyo M, McMaster JS, Gaczynska M, Ploegh HL. A proteolytic system that compensates for loss of proteasome function. Nature 1998;392:618–22.
24. Shumway SD, Miyamoto S. A mechanistic insight into a proteasome-independent constitutive inhibitor κBα (IκBα) degradation and nuclear factor κB (NF-κB) activation pathway in WEHI-231 B-cells. Biochem J 2004;380:173–80.
25. Huang S, DeGuzman A, Bucana CD, Fidler IJ. Nuclear factor-κB activity correlates with growth, angiogenesis, and metastasis of human melanoma cells in nude mice. Clin Cancer Res 2000;6:2573–81.
26. Siwak DR, Shishodia S, Aggarwal BB, Kurzrock R. Curcumin-induced antiproliferative and proapoptotic effects in melanoma cells are associated with suppression of IκB kinase and nuclear factor κB activity and are independent of the B-Raf/mitogen-activated/extracellular signal-regulated protein kinase pathway and the Akt pathway. Cancer 2005;104:879–90.
27. Palombella VJ, Rando OJ, Goldberg AL, Maniatis T. The ubiquitin-proteasome pathway is required for processing the NF-κB1 precursor protein and the activation of NF-κB. Cell 1994;78:773–85.
28. Krappmann D, Scheidereit C. A pervasive role of ubiquitin conjugation in activation and termination of IκB kinase pathways. EMBO Rep 2005;6:321–6.
29. Wang KK, Nath R, Posner A, et al. An α-mercaptoacrylic acid derivative is a selective nonpeptide cell-permeable calpain inhibitor and is neuroprotective. Proc Natl Acad Sci U S A 1996;93:6687–92.
30. Orlowski RZ. Bortezomib and its role in the management of patients with multiple myeloma. Expert Rev Anticancer Ther 2004;4:171–9.
31. Hideshima T, Chauhan D, Richardson P, et al. NF-κB as a therapeutic target in multiple myeloma. J Biol Chem 2002;277:16639–47.
32. Scholzke MN, Potrovita I, Subramaniam S, Prinz S, Schwaninger M. Glutamate activates NF-κB through calpain in neurons. Eur J Neurosci 2003;18:3305–10.
33. Reichrath J, Rech M, Seifert M. Vitamin D-induced apoptosis and melanoma: does calpain represent the major execution protease rather than caspases? J Pathol 2003;201:335–6.
34. Sergeev IN. Genistein induces Ca^{2+}-mediated, calpain/caspase-12-dependent apoptosis in breast cancer cells. Biochem Biophys Res Commun 2004;321:462–7.
35. Nawrocki ST, Carew JS, Pino MS, et al. Bortezomib sensitizes pancreatic cancer cells to endoplasmic reticulum stress-mediated apoptosis. Cancer Res 2005;65:11658–66.

Regulation of Peroxisome Proliferator–Activated Receptor γ Activity by Losartan Metabolites

Michael Schupp, Lucas D. Lee, Nikolaj Frost, Sumaira Umbreen, Boris Schmidt, Thomas Unger, Ulrich Kintscher

Abstract—Two active metabolites of the angiotensin type 1 (AT_1) receptor blocker losartan have been described previously, EXP3174 and EXP3179. Whereas EXP3174 is the main antihypertensive AT_1 receptor–blocking metabolite, the role of EXP3179 is widely unknown. Recently, a subgroup of AT_1 receptor blockers has been identified as ligands for the peroxisome proliferator–activated receptor γ (PPAR-γ). Here we characterize the PPAR-γ–activating properties of the 2 active losartan metabolites. PPAR-γ activity was measured with a chimeric Gal4-DNA–binding domain–hPPARγ-ligand–binding domain (LBD) fusion protein on a Gal4-dependent luciferase reporter system. EXP3179 prominently induced the activation of the PPAR-γ–LBD reaching a maximum at 100 μmol/L with a 7.1±1-fold induction ($P<0.05$ versus vehicle-treated cells). Maximum PPAR-γ–LBD activation by EXP3179 reached 51% of the maximum response induced by the full PPAR-γ agonist pioglitazone, identifying EXP3179 as a partial PPAR-γ agonist. EXP3174 did not induce PPAR-γ–LBD activation. EC_{50} values were calculated for PPAR-γ–LBD activity (pioglitazone EC_{50}: 0.88 μmol/L; EXP3179 EC_{50}: 17.1 μmol/L; losartan EC_{50}: >50 μmol/L). Consistent with the activation of PPAR-γ, EXP3179 potently induced 3T3-L1 adipocyte differentiation, a typical PPAR-γ–dependent cell function, and markedly stimulated PPAR-γ target gene expression. EXP3174 failed to regulate differentiation or PPAR-γ target gene expression. The present study characterizes the active losartan metabolite EXP3179 as a partial PPAR-γ agonist. PPAR-γ activation by EXP3179 may help us to understand the beneficial metabolic effects of losartan observed in clinical trials. (***Hypertension*. 2006;47[part 2]:1-4.)**

Key Words: diabetes mellitus ■ insulin resistance ■ angiotensin antagonists

The Losartan Intervention For End point reduction in hypertension (LIFE) study has shown that hypertensive patients receiving the angiotensin type 1 receptor blocker (ARB) losartan have a 25% lower rate of new-onset diabetes than patients treated with the β-blocker atenolol.[1] Although these data suggest a possible antidiabetic action of losartan, the molecular mechanisms are widely unknown.

We and others recently demonstrated that a subset of ARBs, including losartan, induces the activity of a nuclear hormone receptor named peroxisome proliferator–activated receptor γ (PPAR-γ) by partial agonism.[2,3] The direct activation of the ligand-binding domain of PPAR-γ by ARBs is independent of their angiotensin type 1 receptor (AT_1R) blocking actions.[3] PPAR-γ functions as a transcriptional regulator in adipose tissue where it regulates multiple genes involved in lipid and glucose metabolism.[4] Activated by synthetic full agonists like thiazolidinediones/glitazones, PPAR-γ markedly improves whole-body insulin sensitivity resulting in decreased levels of fasting plasma glucose, fasting plasma insulin, and plasma triglycerides.[5] Thus, PPAR-γ activation by ARBs presents a promising molecular mechanism for metabolic actions of these compounds.

Losartan induced PPAR-γ activity only at high concentrations in vitro.[3] Losartan is hepatically metabolized by the cytochrome-P450 pathway and exerts its antihypertensive actions in vivo predominantly by its main metabolite, EXP3174 (Figure 1).[6,7] During hepatic metabolization of losartan, additional active metabolites are produced, including EXP3179 (Figure 1). This metabolite has a significant molecular homology with indomethacin, an antiinflammatory cyclooxygenase (COX) inhibitor, and mediates a variety of AT_1R-independent, pleiotropic functions (eg, inhibition of platelet aggregation, endothelial adhesion molecule expression, etc).[7] Indomethacin has been also identified as an activator of PPAR-γ.[8] Given the structural homology of indomethacin and EXP3179, it is likely that EXP3179 has

Received September 28, 2005; first decision October 11, 2005; revision accepted November 2, 2005.

From the Center for Cardiovascular Research (M.S., L.D.L., N.F., T.U., U.K.), Institute of Pharmacology and Toxicology, Charité-Universitätsmedizin Berlin, Berlin, Germany; Division of Endocrinology, Diabetes, and Metabolism (M.S.), Department of Medicine, University of Pennsylvania School of Medicine, Philadelphia, Pa; and Technical University (S.U., B.S.), Institute for Organic Chemistry and Biochemistry, Darmstadt, Germany.

T.U. has been a member of the advisory boards and speakers bureau of Boehringer, MSD, Abbot, Novartis, Sanofi-Aventis, and Takeda. T.U. has received research grants from Boehringer, MSD, Novartis, and Takeda. U.K. has received research grants from Boehringer, and Glaxo-Smith-Kline. B.S. has received research grants from Novartis and Schering AG.

Correspondence to Ulrich Kintscher, Center for Cardiovascular Research, Institute of Pharmacology and Toxicology, Charité Campus Mitte, Universitätsmedizin Berlin, Hessische Str 3/4, 10115 Berlin, Germany. E-mail ulrich.kintscher@charite.de

Hypertension **is available at http://www.hypertensionaha.org** **DOI: 10.116110.1161/01.HYP.0000196946.79674.8b**

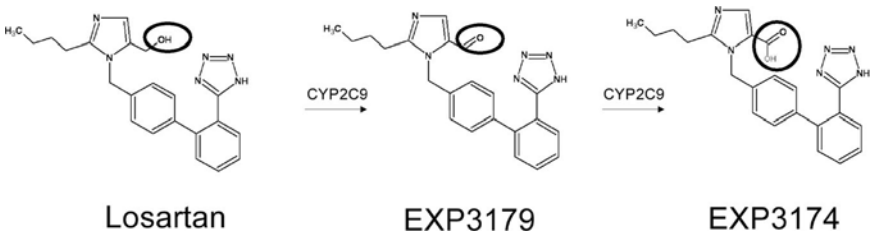

Figure 1. Losartan metabolites. Losartan is actively metabolized in the liver predominantly by the cytochrome P450 isoenzyme CYP2C9. The first oxidation results in the aldehyde EXP3179, which is additionally oxidized to EXP3174.

also PPAR-γ–binding properties. We hypothesized that the PPAR-γ–activating properties of losartan in vivo might be enhanced by its active metabolites and that PPAR-γ activation by losartan metabolites may provide a potential mechanism of the antidiabetic actions of losartan observed in clinical trials.

Methods

Cell Culture

3T3-L1 adipocytes were differentiated as described previously in the absence of 3-isobutyl-1-methylxanthine.[3] After 9 days, Oil-Red-O staining was performed to assess lipid accumulation. COS-7 cells were purchased from American Type Culture Collection.

Synthesis of EXP3179

The in vitro synthesis of EXP3179 has been described previously.[7] In brief, EXP3179 was synthesized from losartan by incubation with $RuCl_3$ and H_2O_2 in MeCN followed by liquid chromatography purification.

Transfection and Luciferase Assay

Transient transfection and luciferase assays were performed as described previously.[3] COS-7 cells were transfected using Lipofectamine 2000 (Invitrogen) with pGal4-human [h] PPARγDEF (hPPAR-γ ligand-binding domain [LBD] fused to Gal4 DBD) and pGal5-TK-pGL3 kindly provided by Bart Staels (UR 545 INSERM), and 10 ng pRL-CMV, a renilla luciferase control reporter vector. After 4 hours, transfection medium was replaced by 10% FBS DMEM plus the indicated compounds or vehicle (dimethylsulfoxide), and luciferase activity was measured after 24 hours.

Quantitative Real-Time PCR

Real-time PCR was performed as described previously with an ABI 7000 sequence detection system.[3] Day-8 adipocytes were serum starved overnight, incubated with compounds for 24 hours, and RNA was isolated. Mouse 18S ribosomal RNA was chosen as endogenous controls (housekeeping genes).

Statistical Analysis

ANOVA and *t* test were performed for statistical analysis as appropriate. Statistical significance was designated at $P<0.05$. Values are expressed as mean±SD.

Results

EXP3179 Enhances 3T3-L1 Adipocyte Differentiation

To examine whether losartan metabolites regulate a PPAR-γ–mediated cell function, differentiation of 3T3-L1 adipocytes was studied in the presence and absence of losartan, EXP3174, EXP3179, and pioglitazone. EXP3179 (10 μmol/L) potently promoted 3T3-L1 adipocyte differentiation as indicated by an increased lipid accumulation assessed with Oil-Red-O staining (Figure 2A and 2B). In similar concentrations, losartan (10 μmol/L) weakly induced lipid accumulation, and the losartan metabolite EXP3174 had no effect (Figure 2A and 2B). Concentration-response experiments revealed that EXP3179-mediated 3T3-L1 adipocyte differentiation started between 1 and 10 μmol/L (Figure 2B). Losartan markedly enhanced the differentiation process only at high concentrations (100 μmol/L; Figure 2B).

EXP3179 Induces PPAR-γ Target Gene Expression

Consistent with the stimulation of adipocyte differentiation, EXP3179 (10 μmol/L) induced mRNA expression of the adipogenic marker and PPAR-γ target gene, adipose protein 2, in 3T3-L1 adipocytes (Figure 3A). Losartan and EXP3174 at 10-μmol/L concentrations had no effect on adipose protein 2 mRNA expression.

A specific characteristic of agonists for PPAR-γ is the downregulation of the receptor on mRNA and/or the protein

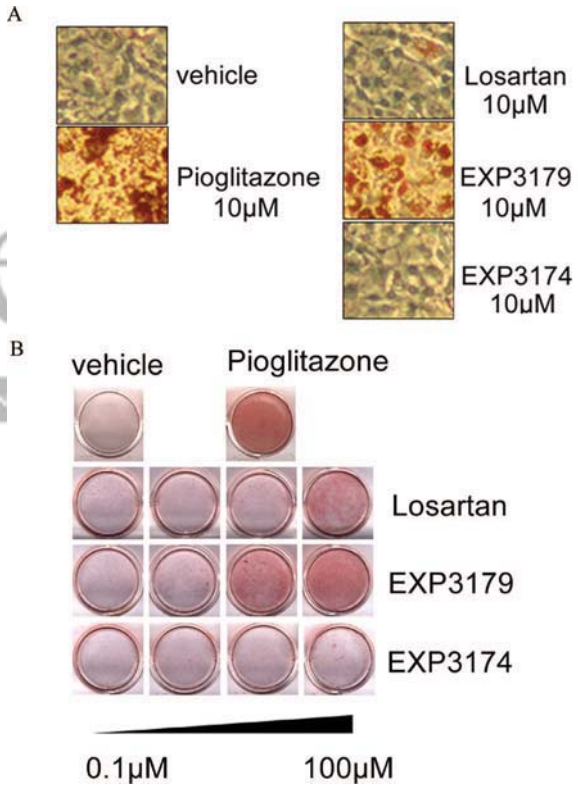

Figure 2. EXP3179 enhances 3T3–L1 adipocyte differentiation. After 9 days differentiation±the indicated compounds, 3T3–L1 cells were stained with Oil Red-O, and representative photographs were taken under phase contrast microscopy. (A) Representatives of 3 separate experiments are presented using ×100 magnification. Brown-gold color staining represents lipid accumulation. (B) Representatives of 3 separate experiments are presented. Red color staining represents lipid accumulation.

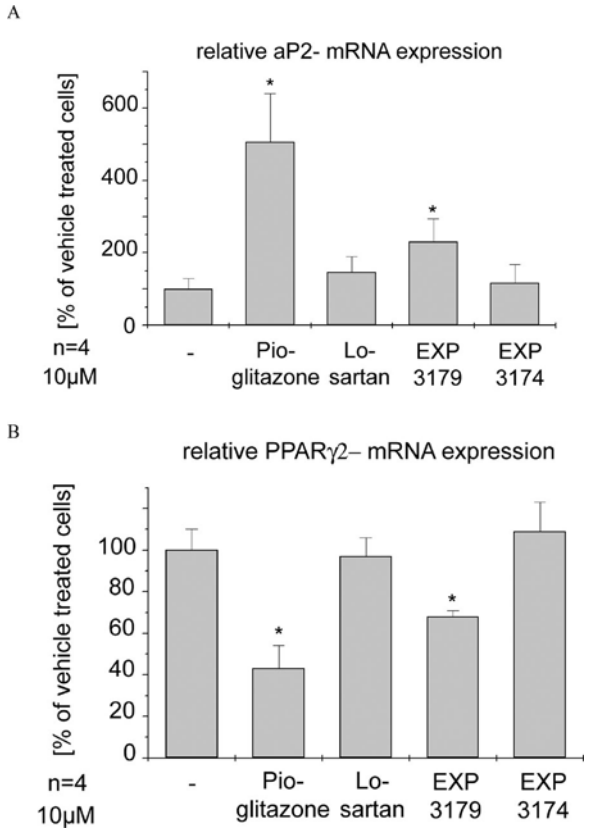

Figure 3. EXP3179 induces PPAR-γ target gene expression. Quiescent day-8 adipocytes were incubated with compounds for 24 hours, and RNA was isolated to measure adipose protein 2 (A) and PPARγ2 (B) expression using real-time PCR. Expression was normalized to 18S expression. Experiments were repeated 4 times, and results are presented as percentage from vehicle-treated cells. Mean±SD is shown. *$P<0.05$ vs vehicle-treated cells.

level in adipocytes on ligand activation in an autoregulatory manner.[9] To additionally characterize EXP3179 as a PPAR-γ activator, we studied the regulation of PPAR-γ2 mRNA expression in 3T3-L1 adipocytes under stimulation with losartan metabolites. In line with pioglitazone-mediated PPAR-γ downregulation, EXP3179 significantly downregulated PPAR-γ2 mRNA expression in 3T3-L1 adipocytes, whereas losartan and EXP3174 had no effect (Figure 3B).

EXP3179 Activates the PPAR-γ Ligand-Binding Domain

To prove that EXP3179 activates PPAR-γ, we assessed its ability to directly activate the PPAR-γ LBD by using a chimeric Gal4-DBD-hPPARγ-LBD fusion protein on a Gal4-dependent luciferase reporter. EXP3179 prominently induced the activation of the PPAR-γ LBD reaching a maximum at 100 µmol/L with a 7.1±1-fold induction ($P<0.05$ versus vehicle-treated cells; Figure 4). Maximum PPAR-γ LBD activation by EXP3179 reached 51% of the maximum response induced by the full PPAR-γ agonist pioglitazone, identifying EXP3179 as a partial PPAR-γ agonist (Figure 4). EXP3174 did not induce PPAR-γ LBD activation (Figure 4). EC_{50} values were calculated for PPAR-γ LBD activity (pioglitazone EC_{50}: 0.88 µmol/L; EXP3179 EC_{50}: 17.1 µmol/L; and losartan EC_{50}: >50 µmol/L).

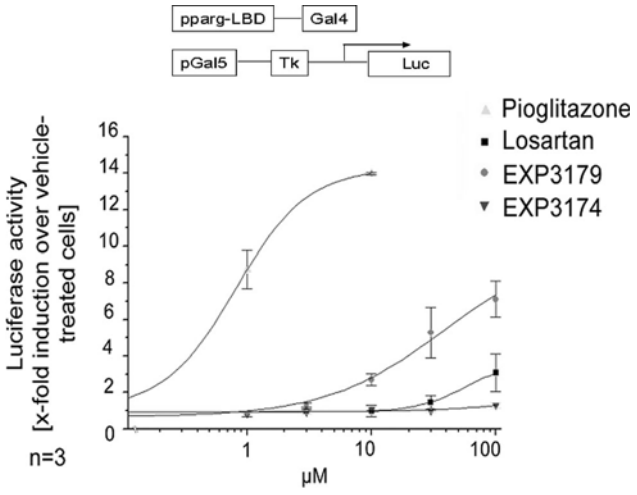

Figure 4. EXP3179 activates the PPAR-γ LBD. COS-7 cells were transiently transfected with the pGal4-hPPARγDEF and pGal5-Tk-pGL3 reporter followed by stimulation with the indicated compounds. Firefly luciferase activity was measured after 24 hours and normalized with activity of cotransfected renilla luciferase. Experiments were repeated 3 times, and results are presented as mean±SD.

Discussion

This study identifies the active losartan metabolite EXP3179 as a partial PPAR-γ agonist. EXP3179 markedly promotes 3T3-L1 adipocyte differentiation, induces PPAR-γ target gene expression, and directly activates the PPAR-γ LBD. PPAR-γ activation by EXP3179 may provide a mechanism for the beneficial antidiabetic actions of losartan observed in clinical trials.

Losartan is a prodrug that is actively metabolized by the cytochrome P450 isoenzyme CYP2C9 on first liver passage to its main antihypertensive metabolite, EXP3174.[6] EXP3174 is 10-fold to 40-fold more potent compared with losartan and mediates most of the AT_1R-blocking effects of losartan.[6] Recently, an important intermediate aldehyde metabolite of losartan, EXP3179, has been identified. In contrast to EXP3174, EXP3179 has very little AT_1R-blocking activity and has been hypothesized to mediate pleiotropic actions of losartan observed in clinical and animal studies.[6] Kramer et al[7] demonstrated that EXP3179 potently inhibits the expression of endothelial COX-2, thereby exerting potent antiinflammatory actions. In addition, Watanabe et al[10] showed that EXP3179 stimulates endothelial NO synthase phosphorylation and suppresses endothelial cell apoptosis induced by tumor necrosis factor α independent of AT_1R-mediated signaling. The molecular mechanism underlying these pleiotropic EXP3179 actions are unknown. Ligand-activated PPAR-γ exerts potent antiinflammatory actions by inhibiting the action of proinflammatory transcription factors, such as AP-1 and nuclear factor κB.[11] Activation of PPAR-γ has also been shown to repress COX-2 promoter activity and mRNA expression by interacting with the c-jun component of the AP-1 complex.[12] EXP3179-mediated activation of PPAR-γ may, therefore, provide a new mechanism of the observed antiinflammatory actions of this compound.

EXP3179 induced PPAR-γ activation as a partial agonist, which implies the consideration of whether the compound may antagonize the actions of a full glitazone agonist during

cotreatment. We performed experiments with another PPAR-γ–activating ARB, telmisartan, in the absence and presence of pioglitazone analyzing the activation of the PPAR-γ LBD in vitro (M. Schupp and U. Kintscher, unpublished data, 2005). These results demonstrated that telmisartan attenuates pioglitazone-induced PPAR-γ activation only at concentrations >10 μmol/L, a concentration that is usually not achieved in patients treated with antihypertensive doses. Because telmisartan is the most potent PPAR-γ–activating ARB, antagonistic actions of these substances on glitazone-induced PPAR-γ activation are unlikely to play a role in vivo or in clinical routine. Furthermore, we demonstrated recently that PPAR-γ–activating ARBs, such as telmisartan and irbesartan, act like selective PPAR-γ modulators compared with the full agonist pioglitazone involving distinct PPAR-γ coactivator binding and induction of distinct gene expression profiles in adipocytes.[13] EXP3179 behaves similar to telmisartan and irbesartan in differentiation assays, adipocytic gene regulation, and transactivation assays, which implicates that EXP3179 may also exert selective PPAR-γ modulator activity.

In clinical trials, losartan has been shown to mediate prominent antidiabetic actions, such as a marked reduction of new-onset diabetes.[1,14,15] The molecular mechanism of these metabolic actions is still far from being understood. It is now well known that blockade of AT_1R results in multiple beneficial effects on insulin and glucose metabolism mediated via an improvement of muscular and pancreatic blood flow or an inhibition of deleterious angiotensin II actions on insulin signaling.[14] We and others recently demonstrated that certain ARBs act like activators of PPAR-γ, which might contribute to their antidiabetic effects.[2,3] However, because PPAR-γ activation by losartan was only achieved at very high concentrations, it appears unlikely that PPAR-γ is responsible for the antidiabetic actions of this compound.[3] In contrast, the losartan metabolite EXP3179 induced PPAR-γ activation more potently compared with losartan identifying this metabolite as a possible mediator of the antidiabetic properties of losartan.

The question remains as to whether EXP3179-mediated PPAR-γ activation plays a role in the antidiabetic actions of losartan observed in clinical studies. Kramer et al[7] reported that after a single oral dose of losartan (100 mg), maximum serum concentrations of EXP3179 between 0.1 and 1 μmol/L were achieved. In the present study, PPAR-γ–mediated adipocyte differentiation, as well as activation of the PPAR-γ LBD by EXP3179, started between 1 and 10 μmol/L. In consideration of the high lipophilicity of EXP3179 rendering it receptive for tissue accumulation and in consideration of an additional increase of serum levels under chronic losartan treatment, EXP3179 concentrations required for PPAR-γ activation may well be reached under losartan treatment. However, rapid hepatic metabolization of EXP3179 has to be taken into account, and additional studies are required to assess whether stable serum and tissue concentrations of EXP3179 are achieved to activate PPAR-γ in patients treated with different doses of losartan.

Perspectives

PPAR-γ activation by EXP3179 may provide a new mechanism of antidiabetic actions induced by losartan. In addition, the identification of an additional PPAR-γ–activating compound with a chemical structure equal to ARBs helps us to understand the characteristic of such substances and supports the development of new dual ARB/PPAR-γ ligands for the treatment of patients experiencing hypertension, insulin resistance, or diabetes.

Acknowledgments

We thank Merck (Rahway, NJ) for kindly providing losartan. T.U. and U.K. are supported by the Deutsche Forschungsgemeinschaft (GK 754). We thank Bart Staels for kindly providing constructs.

References

1. Dahlof B, Devereux RB, Kjeldsen SE, Julius S, Beevers G, Faire U, Fyhrquist F, Ibsen H, Kristiansson K, Lederballe-Pedersen O, Lindholm LH, Nieminen MS, Omvik P, Oparil S, Wedel H. Cardiovascular morbidity and mortality in the Losartan Intervention For Endpoint reduction in hypertension study (LIFE): a randomised trial against atenolol. *Lancet*. 2002;359:995–1003.
2. Benson SC, Pershadsingh HA, Ho CI, Chittiboyina A, Desai P, Pravenec M, Qi N, Wang J, Avery MA, Kurtz TW. Identification of telmisartan as a unique angiotensin II receptor antagonist with selective PPARgamma-modulating activity. *Hypertension*. 2004;43:993–1002.
3. Schupp M, Janke J, Clasen R, Unger T, Kintscher U. Angiotensin type 1 receptor blockers induce peroxisome proliferator-activated receptor-gamma activity. *Circulation*. 2004;109:2054–2057.
4. Lee CH, Olson P, Evans RM. Minireview: lipid metabolism, metabolic diseases, and peroxisome proliferator-activated receptors. *Endocrinology*. 2003;144:2201–2207.
5. Staels B, Fruchart JC. Therapeutic roles of peroxisome proliferator-activated receptor agonists. *Diabetes*. 2005;54:2460–2470.
6. Schmidt B, Schieffer B. Angiotensin II AT1 receptor antagonists. Clinical implications of active metabolites. *J Med Chem*. 2003;46:2261–2270.
7. Kramer C, Sunkomat J, Witte J, Luchtefeld M, Walden M, Schmidt B, Tsikas D, Boger RH, Forssmann WG, Drexler H, Schieffer B. Angiotensin II receptor-independent antiinflammatory and antiaggregatory properties of losartan: role of the active metabolite EXP3179. *Circ Res*. 2002;90:770–776.
8. Lehmann JM, Lenhard JM, Oliver BB, Ringold GM, Kliewer SA. Peroxisome proliferator-activated receptors alpha and gamma are activated by indomethacin and other non-steroidal anti-inflammatory drugs. *J Biol Chem*. 1997;272:3406–3410.
9. Hauser S, Adelmant G, Sarraf P, Wright HM, Mueller E, Spiegelman BM. Degradation of the peroxisome proliferator-activated receptor gamma is linked to ligand-dependent activation. *J Biol Chem*. 2000;275:18527–18533.
10. Watanabe T, Suzuki J, Yamawaki H, Sharma VK, Sheu SS, Berk BC. Losartan metabolite EXP3179 activates Akt and endothelial nitric oxide synthase via vascular endothelial growth factor receptor-2 in endothelial cells: angiotensin II type 1 receptor-independent effects of EXP3179. *Circulation*. 2005;112:1798–1805.
11. Pascual G, Fong AL, Ogawa S, Gamliel A, Li AC, Perissi V, Rose DW, Willson TM, Rosenfeld MG, Glass CK. A SUMOylation-dependent pathway mediates transrepression of inflammatory response genes by PPAR-gamma. *Nature*. 2005;437:759–763.
12. Subbaramaiah K, Lin DT, Hart JC, Dannenberg AJ. Peroxisome proliferator-activated receptor gamma ligands suppress the transcriptional activation of cyclooxygenase-2. Evidence for involvement of activator protein-1 and CREB-binding protein/p300. *J Biol Chem*. 2001;276:12440–12448.
13. Schupp M, Gineste R, Clemenz M, Witt H, Janke J, Helleboid S, Hennuyer N, Ruiz P, Unger T, Staels B, Kintscher U. Selective PPARgamma-modulation by AT1-receptor blockers. *Hypertension*. 2005;46:868–869 (abstract).
14. Scheen AJ. Renin-angiotensin system inhibition prevents type 2 diabetes mellitus. Part 2. Overview of physiological and biochemical mechanisms. *Diabetes Metab*. 2004;30:498–505.
15. Scheen AJ. Renin-angiotensin system inhibition prevents type 2 diabetes mellitus. Part 1. A meta-analysis of randomised clinical trials. *Diabetes Metab*. 2004;30:487–496.

EXP3179 Inhibits Collagen-Dependent Platelet Activation via Glycoprotein Receptor-VI Independent of AT_1-Receptor Antagonism: Potential Impact on Atherothrombosis
Grothusen: EXP3179 and platelets

Christina Grothusen MD[1], Sumaira Umbreen[2], Ildiko Konrad[3], Konstantinos Stellos MD[4], Christian Schulz MD[3], Boris Schmidt PhD[2], Elisabeth Kremmer MD[5], Omke Teebken MD[6], Steffen Massberg MD[3], Maren Luchtefeld PhD[1], Bernhard Schieffer MD[1*], Meinrad Gawaz MD[4*]

[1]Abteilung fuer Kardiologie und Angiologie, Medizinische Hochschule Hannover, Germany
[2]Institut fuer Organische Chemie und Biochemie, Technische Universitaet Darmstadt, Germany
[3]Deutsches Herzzentrum und 1. Medizinische Klinik, Technische Universitaet Muenchen, Germany
[4]Abteilung fuer Kardiologie und Angiologie, Medizinische Klinik III, Universitaet Tuebingen, Germany
[5]Institut fuer Molekulare Immunologie, GSF-Nationales Forschungszentrum fuer Umwelt und Gesundheit, Muenchen, Germany
[6]Abteilung fuer Thorax- and Kardiovaskulaere Chirurgie, Medizinische Hochschule Hannover, Germany

[*]Co-contributing senior authors

Corresponding Author:
Bernhard Schieffer, MD,
Abt. fuer Kardiologie und Angiologie,
Medizinische Hochschule Hannover,
Carl-Neuberg-Str. 1, 30625 Hannover, Germany
Phone: +49-511-532-2129,
Fax: +49-511-532 6473,
e-mail: Schieffer.Bernhard@mh-hannover.de

Total word count: 4933
Abstract: 189
Figures: 6

Abstract

Objective: Thrombus formation following atherosclerotic plaque rupture critically involves the platelet collagen receptor glycoprotein (GP)VI. We investigated the impact of EXP3179, an active metabolite of the angiotensin II type 1 (AT_1)-receptor antagonist Losartan (LOS) on GPVI - dependent platelet activation.

Methods and Results: EXP3179 and LOS but not EXP3174 - the major AT_1-receptor blocking metabolite of LOS - dose-dependently inhibited collagen-I and GPVI-dependent platelet aggregation analysed by optical aggregometry ($p<0.01$). Platelet activation was further determined by flow cytometry measuring the expression of platelet PAC-1, an epitope of the activated fibrinogen-receptor complex. Both, EXP3179 and LOS inhibited collagen-I and GPVI-dependent PAC-1 expression ($p<0.01$). EXP3174 reduced collagen-I ($p<0.05$) but not GPVI-dependent PAC-1 expression. EXP3179 and LOS but not EXP3174 decreased the adhesion of GPVI-receptor expressing chinese hamster ovarian (CHO)-cells on collagen-I under shear conditions as analysed by flow chamber ($p<0.01$). EXP3179 also reduced human atherosclerotic plaque material-induced platelet aggregation ($p<0.01$) *in vitro* and murine platelet adhesion after acute vessel injury *in vivo* as determined by intravital microscopy ($p<0.01$).

Conclusion: EXP3179 acts as a specific inhibitor of the platelet collagen receptor GPVI independent of AT_1-receptor antagonism. Further investigations may clarify its individual potential as a novel pharmacological approach to specifically inhibit atherothrombotic events by GPVI-receptor blockade.

Condensed Abstract

This study investigated the impact of EXP3179, an active metabolite of Losartan on collagen-induced platelet activation via the GPVI-receptor, which is involved in platelet adhesion to atherosclerotic lesions. EXP3179 inhibits collagen-dependent platelet activation by GPVI-receptor blockade independent of AT_1-receptor antagonism, suggesting a novel role for EXP3179 as a platelet-inhibitory agent.

Keywords: EXP3179, platelets, collagen, GPVI-receptor, atherothombosis

Introduction

Occlusive arterial thrombosis following atherosclerotic plaque rupture represents the major pathophysiological mechanism underlying acute coronary syndromes (ACS) or cerebrovascular events, i.e. stroke.[1] Atherosclerotic plaque rupture injures the integrity of the vascular wall and leads to exposure of highly pro-coagulatory extracellular matrix (ECM) components.[2,3] These include collagen-I, a major element of the structurally altered ECM in atherosclerotic vessels.[4-6] The importance of collagen-platelet interactions via the platelet collagen receptor glycoprotein (GP)VI for arterial thrombus formation following vessel injury has recently been recognized by experimental and clinical data. In this regard, GPVI seems to be crucial for thrombus formation in response to platelet contact with human atherosclerotic plaque material *ex vivo* and *in vivo* at sites of murine arterial vascular injury.[7,8,9] Subsequently, platelet GPVI-receptor surface expression was found to be elevated in patients with ACS.[10] Thus, blockade of GPVI-receptor activation may represent a novel pharmacological target to inhibit atherothrombotic events following atherosclerotic plaque rupture.

EXP3179 was originally identified as an active metabolite of the angiotensin II type 1 (AT_1)-receptor antagonist Losartan (LOS), which is produced during the hepatic metabolization of LOS by the cytochrome-P450 pathway (figure 1A).

We recently reported that EXP3179 is detectable in patients after LOS administration and inhibits platelet activation, even though the underlying mechanisms remained unclear.[11] Current observations from other groups revealed, that EXP3179 activates the endothelial nitric oxide synthase (eNOS) and acts as a peroxisome proliferator-activated receptor (PPAR)-gamma agonist.[11-13] So far, the potentially beneficial effects of EXP3179 have only been investigated in concomitance and dependence of LOS treatment. In contrast, we here postulated that EXP3179 might possess an individual pharmacological potential independent of LOS application and its impact on the AT_1-receptor. Therefore, we analysed the effects of EXP3179, LOS and EXP3174 - the main metabolite of LOS and specific AT_1-receptor antagonist - on collagen-I and GPVI-receptor-dependent platelet activation, adhesion and aggregation and evaluated the impact of EXP3179 on acute platelet adhesion to the injured arterial vessel wall *in vivo.*

Materials and Methods

Synthesis of EXP3179

The ^{1}H- and ^{13}CNMR spectra were recorded on a Bruker AC 300 spectrometer at 300 (75). Chemical shifts are reported as % values (ppm) downfield from Me_4Si. Mass spectrometry was performed on a Bruker-Franzen Esquire LC mass spectrometer. Flash column chromatography was carried out using Merck silica gel 60 (40-63 and 15-40 μm) and 60G (5-40 μm). Thin-layer chromatography (TLC) was carried out using aluminum sheets precoated with silica gel 60 F_{254} (0.2 mm; Merck, Germany). Chromatographic spots were visualized by UV and/or spraying with an acidic, ethanolic solution of *p*-anisaldehyde or an ethanolic solution of ninhydrin followed by heating. IBX (2-iodoxybenzoic acid). All commercial chemicals were used without further purification. EXP3179 was synthesized by a modified protocol, which provides higher yields than the previously reported methods.[11,13] Losartan (0.422 g, 1 mmol) was oxidized with IBX (2-iodoxybenzoic acid, 0.321 g, 1.2 mmol) in DMSO (5 mL) at room temperature for 6 h. CH_2Cl_2 (30 mL) was added and the solution was washed with water (3 x 30mL), $NaHCO_3$ solution (3 x 30 mL, sat.), and brine (1 x 30 mL). The solvent was removed after drying (Na_2SO_4) *in vacuo* to yield the product (410 mg, 98%) EXP3179.

Synthesis of EXP3174 via EXP3179

A mixture of 0.147 g (0.35 mmol) of EXP3179 and 0.287 g (3.3 mmol) of activated manganese dioxide in 2 ml of H_2O was refluxed for 78 hrs. The reaction was monitored by TLC ($CHCl_3$/MeOH/CH_3COOH 95/5/0.5). Excess of MnO_2 was filtered, the solvent was removed under reduced pressure and the residue was purified by acid base workup. EXP3174 (200 mg, yield 56 %)[14,15]

EXP3179, Losartan and EXP3174 Stock Solutions

EXP3179 was dissolved in 0.05% DMSO (Sigma-Aldrich, USA), 9.95% Tris-HCl and diluted in phosphate buffered saline (PBS, pH 7.4, free of Ca^{2+} and Mg^{2+}, Sigma-Aldrich, USA). Losartan was dissolved in PBS (pH 7.4, free of Ca^{2+} and Mg^{2+}, Sigma-Aldrich, USA). EXP3174 was dissolved in 10% Tris-HCl and diluted in PBS (pH 7.4, free of Ca^{2+} and Mg^{2+}, Sigma-Aldrich, USA).

Blood Samples

Human peripheral venous blood samples were taken with a loose tourniquet to avoid artefacts through a short venous catheter inserted into the forearm of healthy volunteer donors, who had not taken any medication known to interfere with platelet activation for at least 14 days.

Aggregometric Analysis

Platelet aggregation was evaluated by optical aggregometry as described previously.[16] After adjustment to a total platelet count of $2x10^8$/mL, Platelet-rich plasma (PRP) was incubated with varying doses of EXP3179, LOS, EXP3174 or the corresponding solvents for 15 min. Collagen (type)-I (Probe&Go, Germany) or 4C9 (provided by the GSF-research centre for Environment and Health GmbH, Institute for molecular Immunology, Munich, Germany), a monoclonal GPVI-receptor stimulating antibody were added in varying concentrations to induce platelet

activation. As reported previously, 4C9 detects the GPVI-receptor on the platelet surface.[3] In addition, adenosin-5`-diphosphate (ADP, 5 µmol/L; Probe&Go, Germany) or thrombin-receptor-activating-peptide (TRAP) (25 µmol/L; Sigma-Aldrich, USA) were used to induce platelet activation. To evaluate the impact of EXP3179 on atherosclerotic plaque material-induced platelet aggregation, we followed a protocol recently published by Penz et al.[9] Patient consent was obtained as approved by the Institutional Ethics Committee. For experiments with murine PRP, samples were pooled. Maximal aggregation at 5 min was used as measurement of aggregation.

Flow Cytometry

Evaluation of the surface expression of platelet membrane glycoproteins was performed by immunolabeling followed by flow cytometry analysis as described previously.[17] In brief, PRP (adjusted to $2x10^8$ platelets/mL) was incubated with varying doses of EXP3179, LOS, EXP3174 or the corresponding solvents for 30 min. followed by incubation with varying dosages of 4c9 or collagen-I and PAC-1 antibody, an epitope of the activated fibrinogen receptor complex (anti-PAC-1 FITC, Becton Dickinson, USA) for 30 min. Samples were fixated with 0.5% paraformaldehyde and analysed within 2 hours. 10,000 events were analysed. Specific antibody binding was expressed as mean intensity of immunofluorescence.

Flow Chamber

ACD (acid citrate dextrose)-anticoagulated whole blood samples were obtained as described previously.[7] Coverslips were coated with collagen-I (20 µg/mL). Platelets were perfused through a flow chamber (Oligene, Germany) mounted on the stage of an Axiovert 100 (Zeiss, Jena, Germany) microscope at high shear rate (1000 sec^{-1}).[18] Images were taken randomly and evaluated offline using a computer-assisted image analysis program (Cap Image 7.1; Zeintl, Germany). The duration of one set of experiments was limited to one hour in order to preserve platelet reactivity. To investigate the impact of EXP3179, LOS and EXP3174 on GPVI-receptor mediated cell adhesion on collagen-I under shear conditions, the Flp-In™ system (Invitrogen, Carlsbad, USA) was used as described elsewhere.[7] In short, the Flp-In™ system was used to generate a CHO-cell line stably expressing the human GPVI-receptor. Non-transfected Flp-In™ - CHO-cells served as controls. CHO-GPVI and CHO-cells were cultured using HAM´s F12 containing 10% FCS + 1% penicillin/streptomycin. For culturing the CHO-GPVI cell line 400 µg/mL hygromycin were added. Surface expression of the human GPVI-receptor by CHO-cells was tested by flow cytometry using the anti-GPVI monoclonal antibody 5C4 (see supplementary data, figure 3). Both cell lines were perfused over collagen-I (20 µg/mL) or bovine serum albumin (BSA, 3%) coated glass coverslips in a cell concentration of 500,000/mL at a constant shear rate (1000 sec^{-1}). Experiments were recorded in real time and evaluated off-line using Cap Image software (Cap Image 7.1; Zeintl, Germany).

Intravital Fluorescence Microscopy

For intravital fluorescence microscopy (IVM) of the injured carotid artery, 12 weeks old C57BL6/J mice (Charles River; Sulzfeld, Germany) were anaesthetized by intraperitoneal injection of Midazolam (5 mg/kg bodyweight), Medetomidine (0.5 mg/kg bodyweight) and Fentanyl (0.05 mg/kg bodyweight). Murine platelets were isolated from whole blood samples and labelled with 5 - (and - 6)-carboxyfluorescein diacetate, succimidyl ester (DCF). The final platelet concentration was $2x10^8$ in 500µL PRP. After pre-incubation of murine platelets with either EXP3179 or the diluent (15 min), samples were administered via a jugular catheter. Adhesion of

fluorescent platelets was analysed by in situ video microscopy before and after carotid injury caused by ligature of the common carotid artery for 5 min as described previously.[3] Adherent platelets were measured using a computer-assisted programme and are given per mm^2 (Capimage, Zeintl, Germany). All experiments were approved by the Institutional Animal Care and Use committee.

Statistics

Data are given as mean±SD of at least 3 independent experiments. Student`s t-test was used. Data are given as mean±SD. A p-value <0.05 was considered statistically significant. Statistical analysis was performed using SPSS.

Results

EXP3179 and LOS Dose-Dependently Inhibit Collagen-I Induced Aggregation and Activation of Human Platelets

After incubation of PRP with increasing dosages of EXP3179, LOS, EXP3174 or the appropriate solvent platelet aggregation was induced by stimulation with varying collagen-I concentrations and analysed by optical aggregometry. EXP3179 and LOS similarly and dose-dependently inhibited collagen-I-induced aggregation of human platelets, reaching significant effects at a concentration of 500 μM after stimulation of PRP with 1 μg/mL and 2 μg/mL collagen-I (EXP3179 10±6.2%, LOS 20±9%, each vs PRP 63±9%, p<0.01, n=3-6, Figure 1B). In contrast, EXP3174 did not influence collagen-I dependent platelet aggregation. While LOS has already been reported to inhibit ADP or TRAP-dependent platelet aggregation, we did not find any impact on these parameters after pre-incubation of PRP with EXP3179 (Figure 1C).[Guerra-Cuesta, 1999 #61][Schwemmer, 2001 #62]

Platelet activation leads to a rapid conformational change of the GPIIb-IIIa receptor complex enabling soluble plasmatic fibrinogen binding, which is considered as a major step towards platelet aggregation.[19] The impact of EXP3179 on GPIIb-IIIa activation was evaluated by flow cytometry using the conformation-dependent antibody PAC-1, an epitope of the activated fibrinogen receptor complex.[16] Platelets were pre-incubated with increasing dosages of EXP3179, LOS, EXP3174 or the indicated solvent followed by incubation with varying concentrations of collagen-I (for dose-response experiments see supplementary data, figure 1). EXP3179, LOS and - to a lesser extent EXP3174 - dose-dependently reduced the expression of PAC-1 reaching a maximum effect at a concentration of 500 μM after stimulation of PRP with 5 μg/ml collagen-I (EXP3179 11.5±2, p<0.01, LOS 12.9±1.8, p<0.01, EXP3174 33.75±9.9, p<0.05, each vs stimulated (stim) PRP 65.82±19.3, n=4-7, Figure 1D). No difference between administration of solvent and PRP alone was detected (see supplementary data, figure 1). EXP3179 did not affect TRAP- or ADP - induced PAC-1 expression (data not shown).

EXP3179 Reduces Human Platelet Adhesion on Collagen-I under Shear Conditions

Platelet adhesion under dynamic shear conditions - as present in vivo– can be simulated by using a flow chamber.[20] As reported by other groups, LOS and EXP3174 may influence collagen-dependent adhesion of human platelets under flow.[21] To evaluate the impact of EXP3179 on this parameter, whole blood samples were labelled with rhodamin-6G and incubated with solvent or EXP3179. Platelet adhesion was investigated under constant perfusion over collagen-I coated cover slides. EXP3179 significantly inhibited platelet adhesion evaluated under high shear

rate (1000sec^{-1}) (44.7± 14.4% vs. 100%; p<0.01; n=5; Figure 1E) in comparison to solvent administration. As high shear rates are predominantly present in the arterial branches and birfurcations of the cardiovascular system and may play an important role at sites of atherosclerotic lesions,[20,22] these results indicate an effective inhibition of platelet adhesion by EXP3179 under pathophysiological arterial flow conditions.

EXP3179 and LOS Inhibit Human GPVI-Receptor-dependent Platelet Activation and Aggregation

To further evaluate the potential mechanisms underlying the anti-aggregatory effects of EXP3179 following collagen stimulation, we analysed the impact of EXP3179, LOS and EXP3174 on the activation of the major platelet collagen receptor GPVI. Therefore, human PRP was pre-incubated with EXP3179, LOS or EXP3174 and stimulated with the selective GPVI-receptor activating antibody 4C9, which has been shown to induce platelet activation via GPVI-receptor ligation.[23] EXP3179 and LOS dose-dependently inhibited GPVI-dependent platelet aggregation reaching a maximum effect at a concentration of 500 μM after stimulation of PRP with 0.1 μg/mL 4c9. EXP3174 did not have any detectable influence on this parameter (EXP3179 18.8±4.9%; LOS 20±9.6%, each vs PRP 70.3±1%, each p<0.01, Figure 2A). Furthermore, flow cytometry experiments revealed that the 4C9-dependent platelet activation represented by PAC-1 expression was substantially reduced in the presence of EXP3179 and LOS reaching a maximum effect at a concentration of 500 μM after stimulation of PRP with 0.1 μg/mL 4c9 (see supplementary data for dose-response experiments, figure 2) (EXP3179 25.2±5.8, LOS 33.2±9.7, each vs stim PRP 508.4±18.9, each p<0.01, Figure 2B). EXP3174 did not significantly influence 4c9-dependent platelet activation. We did not detect any difference between administration of solvent and PRP alone (see supplementary data, figure 2).

EXP3179 and LOS Inhibit GPVI-Receptor Dependent Cell Adhesion on Collagen-I under Shear Conditions

To further specify the influence of EXP3179 on GPVI-receptor dependent cell adhesion under shear conditions, GPVI-receptor-expressing CHO cells were used as previously described.[7] EXP3179 and LOS but not EXP3174 (each used in a concentration of 500 μM) significantly inhibited the adhesion of CHO-GPVI cells on collagen-I coated cover slips in comparison to incubation with solvent (see supplementary data, figure 4) or untreated cells (EXP3179 14.3±9 vs 40.9±8.7, p<0.01, LOS 30.1±9.7, p<0.05, each vs 40.9±8.7 untreated CHO-GPVI cells cells/mm^2, n=3, Figure 3). Neither EXP3179 nor LOS influenced the adhesion of control CHO-F cells (see supplementary data, figure 5).

EXP3179 Decreases Human Platelet Aggregation after Stimulation with Human Atherosclerotic Plaque Material

Thrombus formation at sites of atherosclerotic lesions seems to be critically influenced by collagen-induced platelet adhesion via GPVI-receptor activation.[9] Therefore, we investigated the impact of EXP3179 on platelet aggregation in response to components of human carotid atherosclerotic plaques *ex vivo* by aggregometry. After incubation with solvent or EXP3179, PRP was stimulated with homogenized atherosclerotic plaque material from patients who had undergone carotid thrombendarterectomy. EXP3179 significantly inhibited platelet aggregation

following stimulation with human plaque homogenates (18.7±19.8% vs 56.7±16.7%; p<0.01; n=4; Figure 4) compared to solvent.

EXP 3179 Reduces Murine Platelet Aggregation *in vitro* and Platelet Adhesion *in vivo*

Stable murine platelet adhesion and aggregation at sites of acute vessel injury *in vivo* are substantially influenced by GPVI-receptor availability.[3,7] Therefore, we evaluated the impact of EXP3179 on murine platelet aggregation and adhesion. To investigate potential species-specific differences of EXP3179, murine platelet aggregation was first investigated *ex vivo*. As shown for human platelets, EXP3179 significantly inhibited murine platelet aggregation after stimulation with collagen-I in comparison to PBS (data not shown) or solvent administration (25.3±24.8% vs 79.5±7.6%; p<0.01; n=8 animals, PRP was pooled for 3 experiments; Figure 5A). To evaluate the influence of EXP3179 on murine platelet activation *in vivo*, a mouse model of carotid injury was used and platelet adhesion at the site of injury was visualized by intravital fluorescence microscopy, as described previously.[3] Murine DCF-labelled platelets were pre-incubated with EXP3179 or solvent and administered via a venous catheter. Carotid injury was induced by ligature of the common carotid artery as described elsewhere.[3] EXP3179 significantly reduced platelet adhesion to the site of injury in comparison to solvent administration. (Figure 5B, 1061.5±298.1 vs 2047.0±692.2 adherent platelets/mm^2; p<0.01; n=6/group).

Discussion

Here we identify EXP3179 as an individual and selective inhibitor of GPVI-receptor dependent platelet activation and aggregation *in vitro* and *in vivo* independent of AT_1-receptor antagonism.

Acute vessel injury by atherosclerotic plaque rupture exposes pro-coagulatory elements of the subendothelial ECM to circulating platelets, which are instantly activated. Subsequently, occlusive arterial thrombosis may occur and result in ACS or stroke.[1] In this regard, collagen-I is one of the major pro-coagulant ECM components in atherosclerotic vessels, which plays a critical role for stable platelet adhesion at the site of injury.[2] The major platelet collagen receptor is considered to be GPVI as suggested by recent experimental and clinical evidence showing the importance of GPVI-receptor activation in collagen-dependent platelet adhesion and thrombus formation, both *in vitro* and *in vivo*.[3,8,24] Interestingly, activation of GPVI may especially be critical for thrombotic events following atherosclerotic plaque rupture.[9] Thus, inhibition of GPVI-receptor activation may represent a novel pharmacological target in the search of more selective and specific anti-thrombotic agents for the prevention and/or treatment of acute occlusive arterial thrombosis, e.g. myocardial infarction or stroke.

Blockade of the renin-angiotensin system (RAS) by AT_1-receptor antagonists such as LOS effectively reduce the incidence of cardiovascular events as demonstrated by large scale clinical trials.[25,26] This impact seemingly involves the generation of active metabolites, i.e. EXP3179 or EXP3174.[27,11] Based on recent observations which revealed various potentially vasoprotective effects of EXP3179, we hypothesised, that EXP3179 might possess an individual pharmacological potency, which may not only contribute to the beneficial effects of LOS but qualify EXP3179 as an independent candidate for future treatment strategies to prevent acute atherothrombosis. Here, we demonstrate that EXP3179 selectively reduces collagen-dependent human platelet activation, adhesion and aggregation independent of AT_1-receptor antagonism. In this regard, Kalinowski et al. already reported that application of LOS itself impairs collagen-induced platelet aggregation

and adhesion, which was attributed to a release of NO.[21] Indeed, Watanabe et al. recently identified EXP3179 as a potent activator of the eNOS phosphorylation.[12] In platelets, however, the role of eNOS remains controversially discussed. Furthermore, eNOS-associated signalling involves not only collagen-related but also alternative pathways, e.g. thrombin or ADP, both of which were not seen to be influenced by EXP3179 in the present study.[28-30] Instead, we show that EXP3179 markedly inhibited GPVI-receptor-mediated platelet aggregation and activation as determined by platelet PAC-1 expression. Furthermore, EXP3179 - in contrast to the main LOS metabolite EXP3174 - substantially reduced the adhesion of GPVI-receptor expressing CHO-cells on collagen-I under shear conditions confirming the specific impact of EXP3179 on GPVI-receptor function. Although the relevance of GPVI-receptor activation in experimental murine arterial thrombosis has lately been critically discussed,[31] recent observations by Penz et al. again emphasized the importance of collagen-dependent platelet activation via the GPVI-receptor for acute thrombus formation at sites of human atherosclerotic lesions.[9] Therefore, we here investigated - in addition to the *in vitro* experiments - the direct impact of EXP3179 on platelet aggregation induced by human atheromatous plaque material. We were able to demonstrate, that EXP3179 inhibits thrombus formation after stimulation with human plaque material. To evaluate the effect of EXP3179 on platelet adhesion and aggregation *in vivo* we used an established mouse model of carotid injury. In this regard, we - and others - reported that murine thrombus formation in this model crucially depends on GPVI-receptor activation.[3,7] Here, we show, that EXP3179 substantially reduces platelet adhesion in response to vessel injury underlining the impact on GPVI-receptor-mediated platelet activation by EXP3179 also *in vivo.*

Study limitations and Clinical Perspectives

Before the onset of the study presented, the pharmacokinetics and – dynamics of EXP3179 *in vivo* had only been investigated once and in context of a single orally - applied dose of LOS.[11] Thus, we are the first to consider and apply EXP3179 as an individual potential drug. Although we did not observe any signs of acute intoxication or obvious signs of un-specificity (compared to solvent) when using EXP3179 in micromolar concentrations, further studies will be needed to establish a dose-dependent pharmaco-toxicological profile of EXP3179.[13] To summarize, this study describes EXP3179 as a potent inhibitor of collagen-dependent platelet activation, aggregation and adhesion via GPVI *in vitro* and *in vivo.* These results indicate EXP3179 as an individual platelet-inhibitory and potentially vasoprotective agent in the experimental attempt to identify new therapeutic strategies to prevent fatal atherothrombotic cardiovascular events.

Acknowledgments

We would like to thank Sandra Kerstan, Iris Schäfer, Lothar Grote and Mirja Sirisko for their excellent technical support. This work is supported by the Deutsche Forschungsgemeinschaft grant Schie 386/7-2.

Conflict of Interest Disclosure

The authors have nothing to disclose.

References

1. Ruggeri ZM. Platelets in atherothrombosis. *Nat Med*. 2002;8:1227-34.
2. Baumgartner HR. Platelet interaction with collagen fibrils in flowing blood. I. Reaction of human platelets with alpha chymotrypsin-digested subendothelium. *Thromb Haemost*. 1977;37:1-16.
3. Massberg S, Gawaz M, Gruner S, Schulte V, Konrad I, Zohlnhofer D, Heinzmann U, Nieswandt B. A crucial role of glycoprotein VI for platelet recruitment to the injured arterial wall in vivo. *J Exp Med*. 2003;197:41-9.
4. Rekhter MD, Zhang K, Narayanan AS, Phan S, Schork MA, Gordon D. Type I collagen gene expression in human atherosclerosis. Localization to specific plaque regions. *Am J Pathol*. 1993;143:1634-48.
5. Rekhter MD. Collagen synthesis in atherosclerosis: too much and not enough. *Cardiovasc Res*. 1999;41:376-84.
6. Opsahl WP, DeLuca DJ, Ehrhart LA. Accelerated rates of collagen synthesis in atherosclerotic arteries quantified in vivo. *Arteriosclerosis*. 1987;7:470-6.
7. Massberg S, Konrad I, Bultmann A, Schulz C, Munch G, Peluso M, Lorenz M, Schneider S, Besta F, Muller I, Hu B, Langer H, Kremmer E, Rudelius M, Heinzmann U, Ungerer M, Gawaz M. Soluble glycoprotein VI dimer inhibits platelet adhesion and aggregation to the injured vessel wall in vivo. *Faseb J*. 2004;18:397-9. Epub 2003 Dec 4.
8. Nieswandt B, Watson SP. Platelet-collagen interaction: is GPVI the central receptor? *Blood*. 2003;102:449-61. Epub 2003 Mar 20.
9. Penz S, Reininger AJ, Brandl R, Goyal P, Rabie T, Bernlochner I, Rother E, Goetz C, Engelmann B, Smethurst PA, Ouwehand WH, Farndale R, Nieswandt B, Siess W. Human atheromatous plaques stimulate thrombus formation by activating platelet glycoprotein VI. *Faseb J*. 2005;19:898-909.
10. Bigalke B, Lindemann S, Ehlers R, Seizer P, Daub K, Langer H, Schonberger T, Kremmer E, Siegel-Axel D, May AE, Gawaz M. Expression of platelet collagen receptor glycoprotein VI is associated with acute coronary syndrome. *Eur Heart J.* 2006;27:2165-9. Epub 2006 Aug 21.
11. Kramer C, Sunkomat J, Witte J, Luchtefeld M, Walden M, Schmidt B, Tsikas D, Boger RH, Forssmann WG, Drexler H, Schieffer B. Angiotensin II receptor-independent antiinflammatory and antiaggregatory properties of losartan: role of the active metabolite EXP3179. *Circ Res*. 2002;90:770-6.
12. Watanabe T, Suzuki J, Yamawaki H, Sharma VK, Sheu SS, Berk BC. Losartan metabolite EXP3179 activates Akt and endothelial nitric oxide synthase via vascular endothelial growth factor receptor-2 in endothelial cells: angiotensin II type 1 receptor-independent effects of EXP3179. *Circulation.* 2005;112:1798-805.
13. Schupp M, Lee LD, Frost N, Umbreen S, Schmidt B, Unger T, Kintscher U. Regulation of peroxisome proliferator-activated receptor gamma activity by losartan metabolites. *Hypertension.* 2006;47:586-9. Epub 2005 Dec 19.
14. Sanagada V, Fiorino F, Perissutti E, Severino B, Terracciano S, Teixeira C, Caliendo G. A convient synthesis by microwave irradiation of an active metabolite (EXP-3174) of Losartan. *Tetrahedron Letters*. 2003;44:1149-1152.
15. Cresp TMS, F. Tetramethyl-5,7,17,19-tetrakisdehydro[141-annuleno[14]annulene, a Macrocyclic Analog of Naphthalene. *J. Am. Chem. Soc*. 1975;97:4412-4413.
16. Gawaz M, Seyfarth M, Muller I, Rudiger S, Pogatsa-Murray G, Wolf B, Schomig A. Comparison of effects of clopidogrel versus ticlopidine on platelet function in patients undergoing coronary stent placement. *Am J Cardiol*. 2001;87:332-6, A9.
17. Fateh-Moghadam S, Bocksch W, Ruf A, Dickfeld T, Schartl M, Pogatsa-Murray G, Hetzer R, Fleck E, Gawaz M. Changes in surface expression of

platelet membrane glycoproteins and progression of heart transplant vasculopathy. *Circulation*. 2000;102:890-7.

18. Siljander PR, Munnix IC, Smethurst PA, Deckmyn H, Lindhout T, Ouwehand WH, Farndale RW, Heemskerk JW. Platelet receptor interplay regulates collagen-induced thrombus formation in flowing human blood. *Blood*. 2004;103:1333-41. Epub 2003 Oct 16.
19. Fullard JF. The role of the platelet glycoprotein IIb/IIIa in thrombosis and haemostasis. *Curr Pharm Des*. 2004;10:1567-76.
20. Holme PA, Orvim U, Hamers MJ, Solum NO, Brosstad FR, Barstad RM, Sakariassen KS. Shear-induced platelet activation and platelet microparticle formation at blood flow conditions as in arteries with a severe stenosis. *Arterioscler Thromb Vasc Biol*. 1997;17:646-53.
21. Kalinowski L, Matys T, Chabielska E, Buczko W, Malinski T. Angiotensin II AT1 receptor antagonists inhibit platelet adhesion and aggregation by nitric oxide release. *Hypertension.* 2002;40:521-7.
22. Lee RT, Schoen FJ, Loree HM, Lark MW, Libby P. Circumferential stress and matrix metalloproteinase 1 in human coronary atherosclerosis. Implications for plaque rupture. *Arterioscler Thromb Vasc Biol.* 1996;16:1070-3.
23. Cabeza N, Li Z, Schulz C, Kremmer E, Massberg S, Bultmann A, Gawaz M. Surface expression of collagen receptor Fc receptor-gamma/glycoprotein VI is enhanced on platelets in type 2 diabetes and mediates release of CD40 ligand and activation of endothelial cells. *Diabetes*. 2004;53:2117-21.
24. Moroi M, Jung SM. Platelet glycoprotein VI: its structure and function. *Thromb Res*. 2004;114:221-33.
25. Dahlof B, Devereux RB, Kjeldsen SE, Julius S, Beevers G, de Faire U, Fyhrquist F, Ibsen H, Kristiansson K, Lederballe-Pedersen O, Lindholm LH, Nieminen MS, Omvik P, Oparil S, Wedel H. Cardiovascular morbidity and mortality in the Losartan Intervention For Endpoint reduction in hypertension study (LIFE): a randomised trial against atenolol. *Lancet*. 2002;359:995-1003.
26. Dickstein K, Kjekshus J. Effects of losartan and captopril on mortality and morbidity in high-risk patients after acute myocardial infarction: the OPTIMAAL randomised trial. Optimal Trial in Myocardial Infarction with Angiotensin II Antagonist Losartan. *Lancet*. 2002;360:752-60.
27. Schmidt B, Schieffer B. Angiotensin II AT1 receptor antagonists. Clinical implications of active metabolites. *J Med Chem*. 2003;46:2261-70.
28. Randriamboavonjy V, Fleming I. Endothelial nitric oxide synthase (eNOS) in platelets: how is it regulated and what is it doing there? *Pharmacol Rep.* 2005;57:59-65.
29. Trepakova ES, Cohen RA, Bolotina VM. Nitric oxide inhibits capacitative cation influx in human platelets by promoting sarcoplasmic/endoplasmic reticulum Ca2+-ATPase-dependent refilling of Ca2+ stores. *Circ Res.* 1999;84:201-9.
30. Willoughby SR, Stewart S, Holmes AS, Chirkov YY, Horowitz JD. Platelet nitric oxide responsiveness: a novel prognostic marker in acute coronary syndromes. *Arterioscler Thromb Vasc Biol.* 2005;25:2661-6. Epub 2005 Oct 27.
31. Mangin P, Yap CL, Nonne C, Sturgeon SA, Goncalves I, Yuan Y, Schoenwaelder SM, Wright CE, Lanza F, Jackson SP. Thrombin overcomes the thrombosis defect associated with platelet GPVI/FcR{gamma} receptor deficiency. *Blood*. 2006;3:3.

Figure Legends

Figure 1: A: Molecular structure of EXP3179. **B:** Impact of EXP3179, LOS and EXP3174 on collagen-I induced human platelet aggregation. Incubation of PRP with EXP3179, LOS, or appropriate solvent led to a dose-dependent inhibition of collagen-I-induced aggregation of human platelets. A significant effect was observed at a concentration of 500 µM after stimulation of PRP with 1 µg/mL or 2 µg/mL collagen-I. EXP3174 had no impact on this parameter. Data are given as maximal aggregation in % and were analysed by optical aggregometry. Data are mean±SD; *p<0.01 vs PRP/solvent; n=5-8 **C:** EXP3179 in a concentration of 500 µM did not influence TRAP- or ADP-induced platelet aggregation. **D:** Incubation of human PRP with EXP3179, LOS, EXP3174 or appropriate solvent followed by stimulation with collagen-I led to a reduction of platelet PAC-1 expression analysed by flow cytometry. The maximum effect was observed at a concentration of 500 µM after stimulation of PRP with 5 µg/mL collagen. Specific antibody binding was expressed as mean intensity of immunfluorescence. Data are mean±SD; #p<0.05 vs stimulated (stim) PRP; *p<0.01 vs stim. PRP; n=4-7 **E:** Impact of EXP3179 on human platelet adhesion under high shear conditions. Whole-blood samples were incubated with solvent or EXP3179 followed by perfusion (1000sec^{-1}) over collagen-I coated cover slides. EXP3179 significantly inhibited platelet adhesion on collagen-I under shear conditions. Data are given as relative platelet adhesion in %. Data are mean±SD; *p<0.01 vs solvent; n=5

Figure 2: Impact of EXP3179, LOS and EXP3174 on GPVI-receptor-dependent human platelet aggregation and activation **A:** Incubation of PRP with EXP3179, LOS, EXP3174 or appropriate solvent was followed by stimulation with 4C9, a GPVI-receptor-activating antibody. EXP3179 and LOS dose-dependently inhibited GPVI-dependent human platelet aggregation analysed by optical aggregometry. The maximum effect was observed at a concentration of 500 µM after stimulation of PRP with 0.1 µg/mL 4c9. EXP3174 did not affect this parameter. Data are given as maximal aggregation in %. Data are mean±SD; *p<0.01 vs PRP; #p<0.05 vs PRP; n=5-8 **B:** Incubation of human PRP with EXP3179, LOS or appropriate solvent followed by stimulation with 4C9 led to a reduction of platelet PAC-1 expression as analysed by flow cytometry. The maximum effect was observed at a concentration of 500 µM after stimulation of PRP with 0.1µg/mL 4c9. EXP3174 did not have a significant impact on GPVI-dependent PAC-1 expression. Specific antibody binding was expressed as mean intensity of immunfluorescence. Data are mean±SD; *p<0.01 vs stimulated (stim) PRP; n=3-7

Figure 3: Impact of EXP3179, LOS and EXP3174 on GPVI-receptor-dependent cell adhesion under shear conditions. CHO-GPVI or CHO-F cells were incubated with EXP3179, LOS, EXP3174 or appropriate solvent followed by perfusion (1000sec^{-1}) over collagen-I or BSA coated cover slides. Incubation of CHO-GPVI cells with EXP3179 and LOS led to a reduction of cell adhesion on collagen-I matrices under shear conditions. EXP3174 did not influence this parameter. Data are mean±SD; *p<0.01 vs CHO-GPVI adhesion on BSA/glass; **p<0.01 vs CHO-GPVI adhesion on collagen-I; #p<0.05 vs CHO-GPVI adhesion on collagen-I; n=3-7

Figure 4: Impact of EXP3179 on atherosclerotic plaque material-induced platelet aggregation. Incubation of human platelets with EXP3179 led to a significant reduction of atherosclerotic plaque material-induced platelet aggregation in comparison to administration of solvent analysed by optical aggregometry. Data are given as maximal aggregation in %. Data are mean±SD; *p<0.01 vs solvent; n=4

Figure 5: Effects of EXP3179 on murine platelet aggregation *in vitro* and platelet adhesion *in vivo*. **A:** Incubation of murine PRP with solvent or EXP3179 reduced

collagen-I-induced platelet aggregation analysed by optical aggregometry. PRP was pooled, using PRP of 8 animals for n=3 experiments. Data are mean±SD; *p<0.01 vs solvent; n=3 **B:** Intravital fluorescent microscopy after ligature of the common carotid artery showed a reduction of murine platelet adherence at the site of injury after pre-incubation of murine PRP with EXP3179 and application via a venous catheter in comparison to solvent administration *in vivo*. Data are mean±SD; ∗p<0.01 vs solvent; n=6

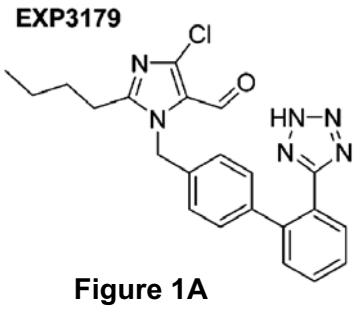

Figure 1A

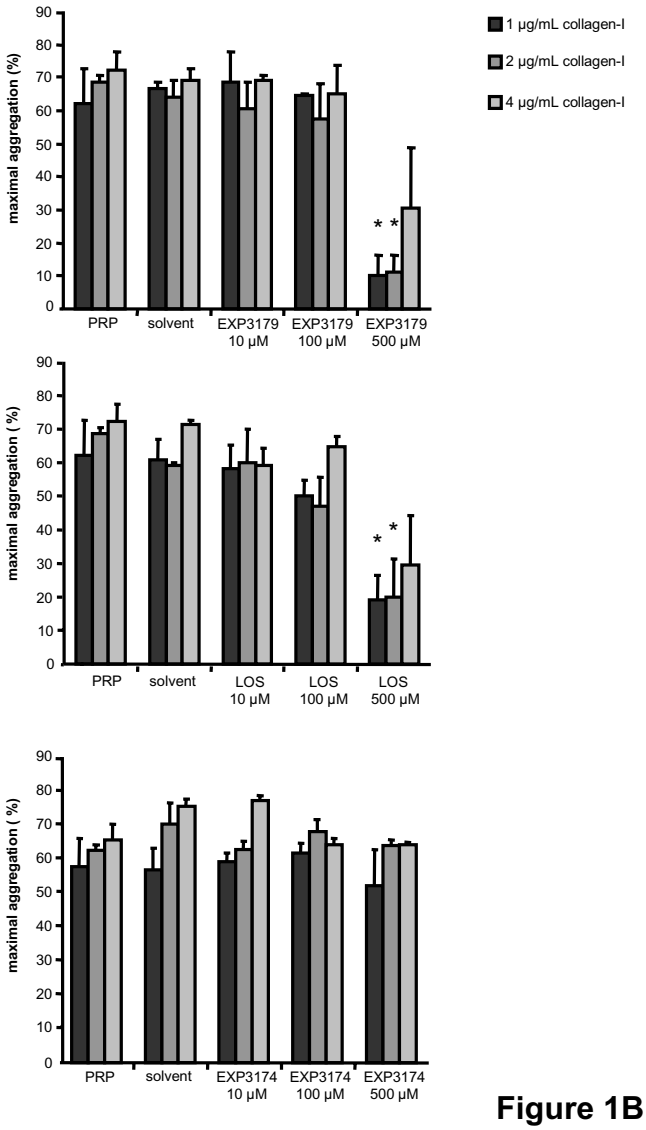

Figure 1B

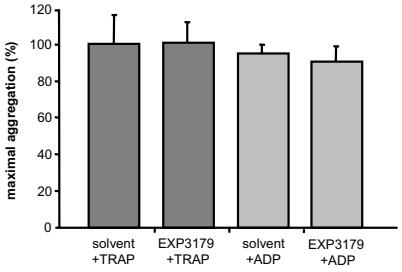

Figure 1C

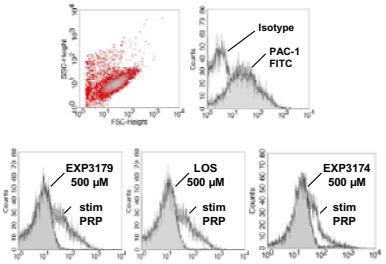

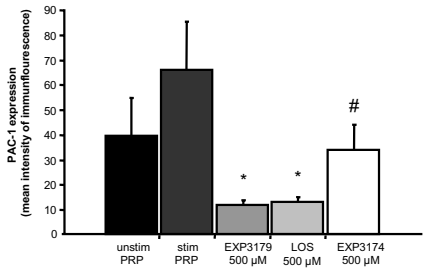

Figure 1D

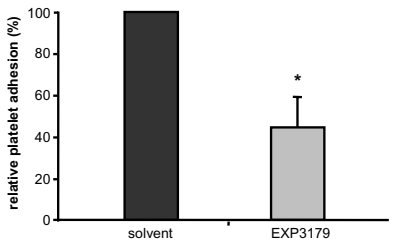

Figure 1E

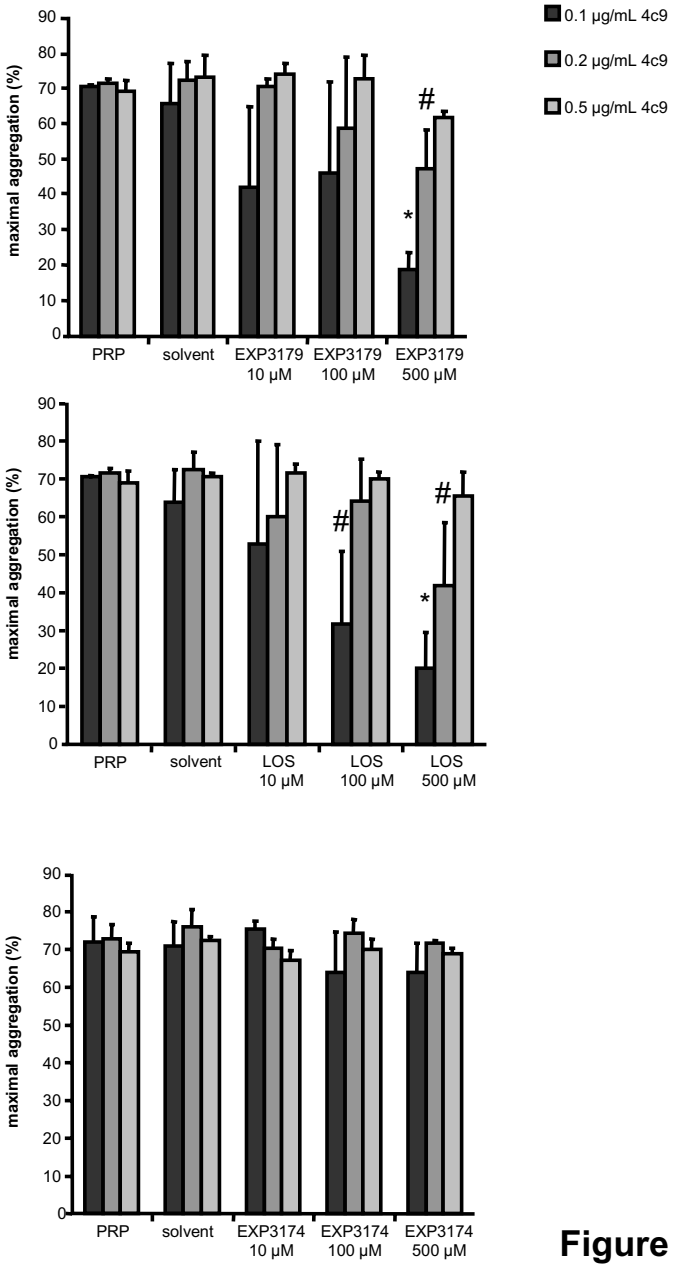
0.1 µg/mL 4c9
0.2 µg/mL 4c9
0.5 µg/mL 4c9
maximal aggregation (%)
PRP
solvent
EXP3179 10 µM
EXP3179 100 µM
EXP3179 500 µM
LOS 10 µM
LOS 100 µM
LOS 500 µM
EXP3174 10 µM
EXP3174 100 µM
EXP3174 500 µM
*
#

Figure 2A

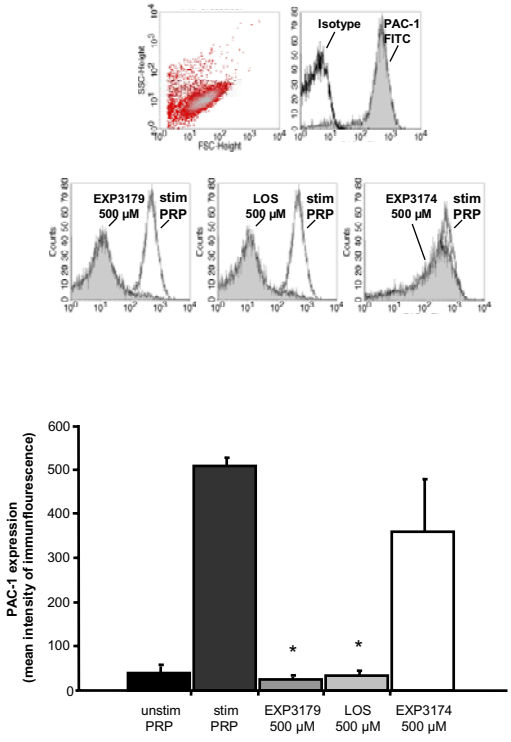

Figure 2B

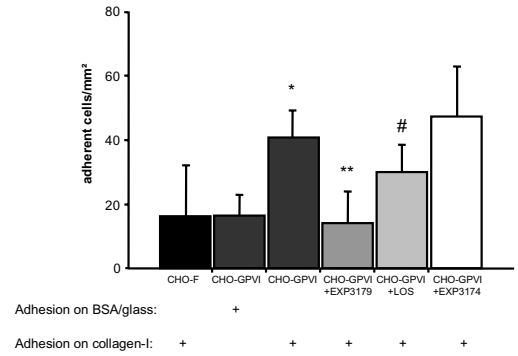

Figure 3

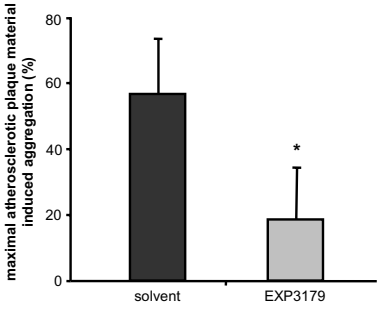

Figure 4

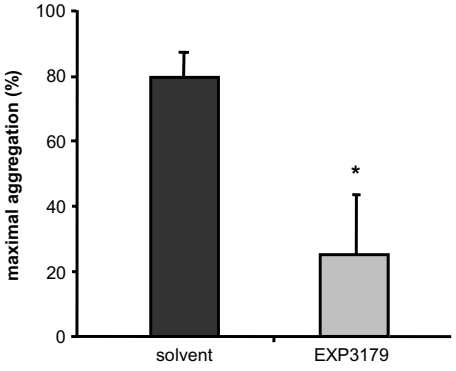

Figure 5A

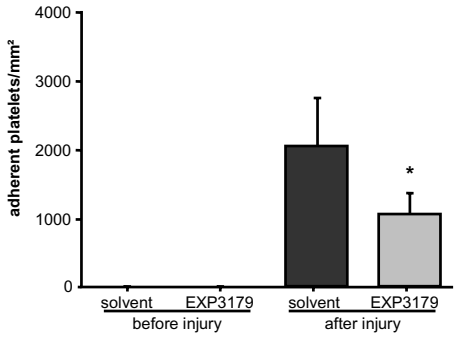

Figure 5B

Title:

Angiotensin receptor type 1 blockade in astroglia decreases hypoxia-induced cell damage and TNF alpha release

Authors:
Lusine Danielyan[1]*, Ali Lourhmati[1], Stephan Verleysdonk[2], Barbara Proksch[1], Sumaira Umbreen[3], Boris Schmidt[3], Christoph H. Gleiter[1]

[1]Department of Clinical Pharmacology, University Hospital of Tuebingen, Tuebingen, Germany

[2]Interfaculty Institute of Biochemistry, University of Tuebingen, Tuebingen, Germany.

[3]Clemens Schoepf-Institute for Organic Chemistry and Biochemistry, Darmstadt, Germany.

*Corresponding Author: L. Danielyan, Department of Clinical Pharmacology, University Hospital of Tuebingen, Otfried-Mueller Strasse 45, 72076 Tuebingen, Germany
Phone: +49-7071-2974926;
Fax: +49-7071-295035;
e-mail: lusine.danielyan@med.uni-tuebingen.de

Running head: Angiotensin receptor type 1 blockade protects astroglia upon hypoxia

Abstract

Despite a multitude of data showing an involvement of the local angiotensin receptor system in neuronal development and survival, little is known about its role for the survival and inflammatory response of astrocytes upon different kinds of injury. Here we show that the AT-R type1 (AT1-R) antagonist losartan and its active metabolite EXP3174 increase the viability of cells in astroglial primary cultures (APC) in a concentration-dependent manner under hypoxic conditions (HC), as determined by LDH release (45±6% decrease). Under HC, APC released 3.5-fold more TNF-alpha than under normoxic conditions (NC). Losartan was capable of decreasing TNF-alpha release under HC (40±15% decrease), alone and in combination with angiotensin II (ATII), while EXP3174 was dependent on ATII for this effect. These data suggest that AT1-R blockade may decrease the susceptibility of astrocytes to hypoxic injury and their propensity to release TNF-alpha. Therefore, AT1-R antagonists may be of therapeutic value during hypoxia-associated neurodegeneration.

Keywords
Hypoxia, angiotensin, neurodegeneration, astrocytes, losartan, EXP3174.

Introduction

Ischemic injury of the brain leads to versatile pathological and defensive processes such as neuronal death, inflammation and activation of microglia as well as astrocytes. Due to their multiple protective features, for instance synthesis of neuroprotective factors such as erythropoietin (1) or vascular endothelial growth factor (2) and maintenance of the extracellular glutamate concentration (3), astrocytes may determine the extent of neuronal damage under hypoxic/ischemic injury. Despite numerous studies demonstrating the critical role of astrocytic apoptosis in the pathogenesis of acute and chronic disorders, such as cerebral ischemia or Alzheimer`s disease (4, 5), the mechanisms regulating astrocytic survival and their capacity to counteract pathological situations are not well understood.

There is increasing evidence for the involvement of the local angiotensin receptor system (ARS) in development, survival and regeneration of neurons. Angiotensin II (ATII) promotes their differentiation and survival in vitro via its receptor subtype 2 (AT2-R) (6) and attenuates hypoxia-induced apoptosis in primary cortical neuronal cultures (7). However, little is known about the role of the ARS in the survival of astrocytes upon different kinds of brain injury. Astrocytes produce ATII and both types of its receptors (AT1-R and AT2-R) (8). ATII promotes the proliferation of different cell types including astrocytes (9, 10), and is upregulated together with its AT2-R after ischemic brain injury (11). The data concerning the effects of ATII during ischemic damage are contradictory: Whilst exogenous application of ATII or AT2-R stimulation decreases the mortality rate in gerbils with unilateral carotid ligation (12, 13) and the long term blockade of AT1-R in rat brain improves the neurological outcome and reduces the infarct volume after experimental ischemia (14), ATII also mediates programmed cell death through AT2-R in different cell types (15). So far, the mechanisms of ATII action on the different CNS cell types and the involvement of its receptor subtypes in protective and pathophysioligical mechanisms during hypoxia-associated injury of the brain are still poorly understood.

Selective AT1-R blockade by losartan and other AT1-R antagonists is widely used in treatment of hypertension, a key factor in the pathophysiology of stroke. Although losartan itself is a potent AT1-R antagonist, its antihypertensive action appears to be primarily due to its active metabolite EXP3174 (16). Polidori et al. (17) have shown a delayed effect of intraperitoneally delivered losartan on central targets of angiotensin action, such as water intake, and that the peripheral administration of EXP3174 inhibited water drinking with higher potency than losartan itself. AT1-R blockade was shown to improve the brain microcirculation and therefore to decrease the vulnerability to brain ischemia and stroke in chronically hypertensive rats (18). It suppresses the inflammation of brain vessels in spontaneously hypertensive rats (19) and prevents stress-induced gastric ulcers, in part by reducing inflammation in the gastric mucosa (20), suggesting the involvement of AT1-R in inflammation connected to different kinds of disorders such as ischemia or stress. Inflammation occurs in early stages of acute and chronic neurodegenerative disorders such as stroke or Parkinson's and Alzheimer's disease (21, 22). A self-amplifying cycle involving brain immune cells (microglia and astrocytes) has been discussed as one of the mechanisms of these inflammation processes. Several attempts have been made to investigate the role of the local angiotensin receptor system in survival of neurons upon different kinds of injury: While losartan is known to increase the protection of neurons provided by ATII against hypoxia- and rotenone-induced cell death (7, 23), the possible cytoprotective and anti-inflammatory effect of AT1-R antagonists on astrocytes remained unexplored prior to this study. Here, the influence of losartan

and its main active metabolite, EXP3174, on hypoxia-induced damage to astrocytes and on their inflammatory response to hypoxic injury has been investigated.

Experimental Procedure

Cell culture

Astroglial primary cultures (APC) were prepared from the brains of newborn Wistar rats as described elsewhere (24). For the cell viability assay, the cells were grown in 96-well microplates (20000 cells/well), whereas for the multiplex assay of interleukins, $1x10^6$ cells were grown in petri dishes (60 mm in diameter). The cells were cultured in Dulbecco's modified Eagle's medium containing 10% foetal calf serum, 100 µg/ml streptomycin sulphate and 100 units/ml penicillin at 37°C in an incubator containing an atmosphere of 10%CO_2 in air until day 8 in vitro (DIV, day in vitro). On DIV 8 the medium was removed and fresh medium containing different supplements was added. The samples were assayed as described below.

Synthesis of EXP3174 via EXP3179

EXP3179 was synthesized by previously reported methods (25, 26) and oxidized further to EXP3174 by activated manganese dioxide in H_2O under reflux for 78 hrs. Excess of MnO_2 was filtered, the solvent was removed *in vacuo* and the residue (EXP3174, 200 mg, yield 56 %) was purified by acid/base workup (27).

Incubation with Losartan, EXP3174 and ATII under normoxic and hypoxic conditions

8 day-old cultures were treated for 48 h either with two different concentrations of losartan (100nM or 1µM) kindly provided by MSD SHARP&DOHME (Haar, Germany) or EXP3174 (100nM, 1µM) alone and in combination with 100nM ATII (Sigma, Deisenhofen, Germany). Losartan and ATII were dissolved in phosphate-buffered saline (PBS), EXP3174 was dissolved in DMSO and further diluted with PBS (0.029% final concentration of DMSO). It was previously shown that the viability of astroglial primary cultures is not affected by this DMSO concentration (28). Cells were cultured for 48h at 37°C either under NC with 10% CO_2 in air or under hypoxic conditions (HC) with 1% O_2, 10% CO_2 and 89% N_2.

Cell viability assay

Cell death induced by culture conditions and hypoxia was measured in terms of LDH activity in supernatants of cells grown in 96-well microplates. The experiments were performed following the protocol accompanying the CytoTox 96® Non-Radioactive Cytotoxicity Assay (Promega, Madison, USA). Briefly, 50 µl of standards or 50 µl of culture supernatant (controls and treated cells) and 50 µl of substrate mix were transferred into a 96-well-plate and incubated for 30 minutes at room temperature. The enzymatic conversion of tetrazolium salt into red formazan product was stopped by 50 µl stop solution. Plates were read out with a SUNRISE Elisa-plate Reader (Tecan, Crailsheim, Germany) at 490 nm. LDH released from the cells was expressed as a percentage of total cellular LDH, which was measured after lysis of the cells by addition of Triton X-100 to a final concentration of 0,1% in each well.

Multiplex analysis of cytokines.

At DIV 8 the medium was removed from cells grown in petri dishes and fresh medium containing either 1µM losartan, 1µM EXP3174 or 1µM EXP3174 and 100nM ATII was added. The cells were then further incubated for 48h under NC or HC. Subsequently, 50 µl from each dishe used for detection of interleukin-4 (IL-4), IL-5, granulocyte-monocyte-colony-stimulating factor (GM-CSF), interferon-gamma (IFNγ) and tumor necrosis factor-alpha (TNFα). The quantification of these cytokines was performed with a Beadlyte® Rat Multi-Cytokine Beadmaster^{TM} Kit (Upstate, Lake Placid, NY) and a Luminex-100 system (Luminex Corporation**,** Austin, TX) according to the manufacturer's instructions. The cytokine concentrations in cell culture supernatants were extrapolated from their respective standard curves by 5-parameter logistic analysis (29).

Statistical analyses

Data presented as mean ± SEM (n=6) were normalized to the mean of corresponding controls (normoxic and hypoxic controls) and converted to percentage of control. *P* <0.05 was considered as significant (***** p<0.05; ****** p<0,01 **, ***** p<0,001). To compare the treated samples with controls, one way ANOVA with Dunett's post comparison test was used.

Results

LDH release as a measure for cell damage was investigated under NC and HC in APC incubated with ATII, Losartan, and EXP3174. Under NC, the application of 100nM and 1µM losartan reduced the release of LDH in a concentration-dependent manner: application of 1µM losartan appeared to be more effective than 100nM losartan (Fig. 1A 100nM L, 1µM L vs. N). The administration of 100nM EXP3174 reduced LDH by 35±11% (Fig. 1A, 100nM EXP), whereas the application of 1µM EXP3174 resulted in a 52±16% decrease of released LDH (Fig. 1A, 1µM EXP). Simultaneous administration of 100nM ATII and 1µM EXP3174 brought no additional decrease of LDH-release (63±14%, Fig 1A, AT+EXP) when compared with the effect of 1µM EXP3174 applied alone (52±16%, Fig. 1A, 1µM EXP). Under HC, 100nM of either EXP3174 or losartan had no effect on release of LDH (Fig. 1B, 100nM L and 100nM EXP) when compared with the hypoxic control (Fig. 1B, H). The reduction in LDH release after application of 1µM losartan (37±19 %, Fig. 1B, 1µM L) was similar to that of either 1µM EXP alone (45±6%, Fig. 1B, 1µM EXP) or EXP3174 in combination with ATII (41±6%, Fig. 1B, AT+1µM EXP).

The concentrations of the inflammatory cytokines IL-4, IL-5, GM-CSF and IFNγ in the cell culture supernatants were far below the detection range (< 14 pg/ml) under both NC and HC. Only TNFα was measurable under NC and 3,5-fold up-regulated upon exposure of the cells to hypoxia (cf. N in Fig. 2A with H in B). The effect of 1µM losartan on TNFα-release under NC (33±10%; Fig. 2A, N+L) was slightly lower than that of 1µM EXP3174 (41±15%; Fig.2A: N+EXP vs. N) in comparison to the normoxic control (N in Fig. 2 A). The effect achieved by simultaneous application of 100nM ATII and 1µM EXP3174 or losartan (N+AT+EXP and N+AT+L in Fig. 2 A) on TNFα-release was similar to the one observed on samples incubated with EXP3174 or losartan alone (Fig. 2A: 63±13% in N+AT+L vs. 33±10% in N+L and 45±10% in N+AT+EXP vs. 41±15% in N+EXP). Under HC, losartan and EXP3174 showed approximately equal efficacies in preventing TNFα release: 1µM losartan or EXP3174 decreased TNFα concentration by 40±15% or 34±20%, respectively (Fig.2 B, H+L vs. H+EXP) when compared to the hypoxic

control (Fig. 2 B, H). Combined application of ATII (100nM) and losartan appeared to decrease TNFα (70±15%, H+AT+L in Fig. 2B) similar to that of ATII with EXP3174 (57±20%, H+AT+EXP in Fig. 2B).

Discussion

Taking into consideration that the AT1-R antagonist losartan is a pharmacologically well characterized therapeutic agent, this study investigated whether this compound and its main active metabolite, EXP3174, may provide a protection of astrocytes against hypoxia-induced cell damage and prevent them from initiating an inflammatory cascade. The data obtained on cell death in terms of LDH release from astroglial cells show that under both NC and HC, losartan and EXP3174 possess a similar protective potency. Astrocytes are known to express all known angiotensin receptor subtypes, namely AT1-R, AT2-R and AT(1-7)-R (30, 31). Their increased survival under losartan and its metabolite may be due to 1) the direct antagonistic effect of losartan and EXP3174 on AT1-R or 2) increased availability of endogenously produced (or exogenously applied) ATII for signal transduction via the remaining receptor subtypes. ATII is known to be produced by astrocytes and to be upregulated under ischemic injury of the brain (11).

Culture condition induces the reactive state of astrocytes, which differs from the resting inactive state typical for these cells in normal brain tissue. This culture-induced activation of astrocytes is entailed by accelerated differentiation and therefore presumably accelerated cell death. It was previously shown that basal release of LDH under normoxic conditions in astroglial cultures is in a range up to 10% of its total intracellular content (32). Results presented here show up to 2,8% LDH release by astroglia under normoxic conditions. Even such a low basal amount of LDH under normoxic conditions in cell culture supernatant was significantly reduced by losartan and EXP3174. Cell culture condition used in this study is the mostly used method over last 20 years for cultivation of astroglial cells. The fact that both compounds (losartan and EXP3174) can increase the viability of cells under well established normoxic culture conditions hint at the possible use of AT1-R blockade as a cell culture supplement capable of creating more physiologic conditions for astroglial cells in vitro. Hypoxia resulted in 30% increase of LDH release. The improvement of astroglial survival under hypoxia after application of losartan or EXP3174 shown here is reconcilable with data demonstrating AT1-R-mediated cell death in myocytes, endothelial cells and blood vessels, in vitro as well as in vivo (33, 34, 35). In contrast to normoxic condition the higher amount of losartan and EXP3174 was needed under hypoxic conditions to improve the survival of astroglial cells: administration of 100nM losartan or EXP3174 revealed no effect on cell survival upon hypoxia. Apparently, AT1-R blockade exerts a direct protective effect on astrocytes during hypoxic injury. Since application of ATII together with EXP3174 was not more efficient in protecting astrocytes from hypoxic cell death than EXP3174 alone, the blockade of AT1-R appears to be more important for survival than the stimulation of AT2-R or A(1-7)-R.

Whether astrocytes can contribute to the local increase of inflammatory factors in response to hypoxia was investigated by multiplex analysis of anti-inflammatory IL-4, IL-5 and GM-CSF, as well as pro-inflammatory IFNγ and TNFα. All these factors have been shown previously to be up-regulated after ischemic injury of the brain (36, 37, 38). IL-4, IL-5, GM-CSF, IFNγ were not detectable under NC or HC. It was previously shown that the exogenous application of IFNγ induces the death of astrocytes via activation of the Jak2/Stat1 pathway in vitro (39). The results

presented here show that even under protracted HC (48h), astrocytes do not respond with measurable changes in their production of IFNγ. The fact that IL-4 release from astrocytes was not influenced by hypoxia is in concordance with the data reported by Park et al. (40) showing that after lipopolysaccharide-induced inflammation of the brain, IL-4 was expressed exclusively in microglia, but not in astrocytes or neurons. Vitcovic et al. (41) have shown that the expression of GM-CSF in astrocytes was not substantially altered by IL-1, an important activator of reactive astrocytosis that is upregulated in astrocytes after hypoxic injury (42). The level of IL-5, an anti-inflammatory cytokine serving as a mitogenic factor for microglia (43) but not for astrocytes (44), was not increased under HC either. The absence of anti-inflammatory IL-4 and 5, as well as pro-inflammatory IFNγ in cell culture supernatants after 48h of hypoxia might hint at a marginal role of these cytokines in the immediate inflammatory response of astrocytes to hypoxia. This suggestion is in agreement with data showing a slight transient increase of IL-4 and IL-5 in microglia and inflammatory leucocytes but not astrocytes during experimental allergic encephalomyelitis (45).

The measured increase in the concentration of TNFα in the cell culture supernatants under HC suggests that the immediate inflammatory response of astrocytes to hypoxia might be reflected by release of this potent pro-inflammatory cytokine. The application of losartan and EXP3174 decreased the amount of released TNFα under NC and HC. This effect was pronounced by concomitant administration of ATII. Therefore, different AT receptors may be involved in the maintenance of the inflammatory response of astrocytes. Presumably, the production of TNFα can be diminished by antagonists at AT1-R and/or stimulation of the other AT receptor subtypes.

The results presented here are somewhat analogous to recently reported data showing the peripheral anti-inflammatory action of the AT1-R antagonist, candesartan, during gastric ulceration (20) to be, in part, reflected by a decreased expression of TNFα in stomach sections of rats under cold-restraint stress.

AT1-R activation stimulates a multitude of signalling pathways including the nuclear factor-kappaB (NF-κB) pathway. In astrocytes the induction of this signal effector leads to early up-regulation and subsequent release of TNFα. The inhibition of the NF-κB transduction pathway was shown to reduce the secretion of TNFα from astrocytes (46). It can be therefore suggested that decrease of TNFα release from astroglia provided by losartan or EXP3174 originates most likely from their activation-reducing effect on NF-κB.

A comparison of the anti-inflammatory effects achieved by losartan and EXP3174 reveals nearly equal efficacy of both compounds under NC and HC, suggesting that losartan delivered to the brain might reduce the susceptibility of astrocytes to hypoxic injury and provide an anti-inflammatory effect even without being converted to EXP3174 in the liver.

In summary, it can be concluded that AT1-R blockade could be of therapeutic benefit during neurodegenerative disorders accompanied by inflammation, such as Alzheimer's disease, Parkinson's disease, stroke and multiple sclerosis due to its anti-inflammatory and vulnerability-reducing effect on astrocytes.

Aknowledgments

We appreciate the support of Microbionix (Regensburg, Germany) in performing of multiplex analysis. This work was supported by "Dr. Karl-Kuhn Stiftung" (Tuebingen, Germany) and MSD SHARP& DOHME GmbH (Haar, Germany).

References

(1) Juul SE, Yachnis AT, Rojiani AM, Christensen RD (1999) Immunohistochemical localization of erythropoietin and its receptor in the developing human brain. Pediatr. Dev. Pathol. 2:148-158.

(2) Beck H, Acker T, Puschel AW, Fujisawa H, Carmeliet P, Plate KH (2002) Cell type-specific expression of neuropilins in an MCA-occlusion model in mice suggests a potential role in post-ischemic brain remodelling. J. Neuropathol. Exp. Neurol. 61: 339-350.

(3) Hansson E, Muyderman H, Leonova J, Allansson L, Sinclair J, Blomstrand F, Thorlin T, Nilsson M, Ronnback L (2000) Astroglia and glutamate in physiology and pathology: aspects on glutamate transport, glutamate-induced cell swelling and gap-junction communication. Neurochem. Int. 37:317-329.

(4) Takuma K, Baba A, Matsuda T (2004) Astrocyte apoptosis: implications for neuroprotection. Prog. Neurobiol. 72:111-127.

(5) Nakase T, Sohl G, Theis M, Willecke K, Naus CC (2004) Increased apoptosis and inflammation after focal brain ischemia in mice lacking connexin43 in astrocytes. Am. J. Pathol. 164:2067-2075.

(6) Rodriguez-Pallares J, Quiroz CR, Parga JA, Guerra MJ, Labandeira-Garcia JL (2004) Angiotensin II increases differentiation of dopaminergic neurons from mesencephalic precursors via angiotensin type 2 receptors. Eur. J. Neurosci. 20:1489-1498.

(7) Grammatopoulos TN, Morris K, Bachar C, Moore S, Andres R, Weyhenmeyer JA (2004) Angiotensin II attenuates chemical hypoxia-induced caspase-3 activation in primary cortical neuronal cultures. Brain. Res. Bull. 62:297-303.

(8) Fogarty DJ, Matute C (2001) Angiotensin receptor-like immunoreactivity in adult brain white matter astrocytes and oligodendrocytes. Glia 35:131-46.

(9) Sumners C, Tang W, Paulding W, Raizada MK (1994) Peptide receptors in astroglia: focus on angiotensin II and atrial natriuretic peptide. Glia 11:110-116.

(10) Wang Z, Rao PJ, Shillcutt SD, Newman WH (2005) Angiotensin II induces proliferation of human cerebral artery smooth muscle cells through a basic fibroblast growth factor (bFGF) dependent mechanism. Neurosci. Lett. 373:38-41.

(11) Kagiyama T, Kagiyama S, Phillips MI (2003) Expression of angiotensin type 1 and 2 receptors in brain after transient middle cerebral artery occlusion in rats. Regul. Pept.110: 241-247.

(12) Fernandez LA, Spencer DD, Kaczmar T Jr (1986) Angiotensin II decreases mortality rate in gerbils with unilateral carotid ligation. Stroke 17:82-85.

(13) Fernandez LA, Caride VJ, Stromberg C, Naveri L, Wicke JD (1994) Angiotensin AT2 receptor stimulation increases survival in gerbils with abrupt unilateral carotid ligation. J. Cardiovasc. Pharmacol. 24:937-940.

(14) Dai WJ, Funk A, Herdegen T, Unger T, Culman J (1999) Blockade of central angiotensin AT(1) receptors improves neurological outcome and reduces expression of AP-1 transcription factors after focal brain ischemia in rats. Stroke 30:2391-2398.

(15) Yamada T, Horiuchi M, Dzau VJ (1996) Angiotensin II type 2 receptor mediates programmed cell death. Proc. Natl. Acad. Sci. U S A. 93:156-160.

(16) Wong PC, Price WA Jr, Chiu AT, Duncia JV, Carini DJ, Wexler RR, Johnson AL, Timmermans PB (1990) Nonpeptide angiotensin II receptor antagonists. XI. Pharmacology of EXP3174: an active metabolite of DuP 753, an orally active antihypertensive agent. J. Pharmacol. Exp. Ther. 255:211-217.

(17) Polidori C, Ciccocioppo R, Pompei P, Cirillo R, Massi M (1996) Functional evidence for the ability of angiotensin AT1 receptor antagonists to cross the blood-brain barrier in rats. Eur. J. Pharmacol. 307:259-267.

(18) Bennai F, Morsing P, Paliege A, Ketteler M, Mayer B, Tapp R, Bachmann S (1999) Normalizing the expression of nitric oxide synthase by low-dose AT1 receptor antagonism parallels improved vascular morphology in hypertensive rats. J. Am. Soc. Nephrol. 10:S104–S115.

(19) Ando H, Zhou J, Macova M, Imboden H, Saavedra JM (2004) Angiotensin II AT1 receptor blockade reverses pathological hypertrophy and inflammation in brain microvessels of spontaneously hypertensive rats. Stroke 35:1726-1731.

(20) Bregonzio C, Armando I, Ando H, Jezova M, Baiardi G, Saavedra JM (2003) Anti-inflammatory effects of angiotensin II AT_1 receptor antagonism prevent stress-induced gastric injury. Am. J. Physiol. 285:G414–G423.

(21) Liu B, Gao HM, Hong J.S (2003) Parkinson's disease and exposure to infectious agents and pesticides and the occurrence of brain injuries: role of neuroinflammation. Environ. Health Perspect. 111:1065-1073.

(22) Heneka MT, Sastre M, Dumitrescu-Ozimek L, Dewachter I, Walter J, Klockgether T, Van Leuven F (2005) Focal glial activation coincides with increased BACE1 activation and precedes amyloid plaque deposition in APP(V717I) transgenic mice. J. Neuroinflammation. 2:22.

(23) Grammatopoulos TN, Ahmadi F, Jones SM, Fariss MW, Weyhenmeyer JA, Zawada WM (2005) Angiotensin II protects cultured midbrain dopaminergic neurons against rotenone-induced cell death. Brain Res. 1045:64-71.

(24) Hamprecht B, Loffler F (1985) Primary glial cultures as a model for studying hormone action. Methods Enzymol. 109:341-345.

(25) Kramer C, Sunkomat J, Witte J, Luchtefeld M, Walden M, Schmidt B, Tsikas D, Boger RH, Forssmann WG, Drexler H, Schieffer B (2002) Angiotensin II receptor-independent antiinflammatory and antiaggregatory properties of losartan: role of the active metabolite EXP3179. Circ Res. 90:770–776.

(26) Schupp M, Lee LD, Frost N, Umbreen S, Schmidt B, Unger T, Kintscher U (2005) CHBPR-Regulation of PPARγ, Activity by Losartan Metabolites. Hypertension 47:586-589.

(27) Santagada V, Fiorino F, Perissutti E, Severino B, Terracciano S, Teixeirab CE, Caliendo G (2003) A convenient synthesis by microwave irradiation of an active metabolite (EXP-3174) of Losartan. Tetrahedron Letters 44:1149–1152.

(28) Danielyan L, Gembizki O, Proksch B, Weinmann M, Morgalla M, Wiesinger H, Buniatian GH, Gleiter CH (2005) The blockade of endothelin A receptor protects astrocytes against hypoxic injury: common effects of BQ-123

anderythropoietin on the rejuvenation of the astrocyte population. Eur. J. Cell. Biol. 84:567-579.

(29) Bates DM, Watts DG (1988) Nonlinear regression analysis and its application, Wiley, New York, pp103-108.

(30) Sumners C, Tang W, Zelezna B, Raizada MK (1991) Angiotensin II receptor subtypes are coupled with distinct signal-transduction mechanisms in neurons and astrocytes from rat brain. Proc. Natl. Acad. Sci. U S A. 88:7567-7571.

(31) Fogarty DJ, Sanchez-Gomez MV, Matute C (2002) Multiple angiotensin receptor subtypes in normal and tumor astrocytes in vitro. Glia 39:304-313.

(32) Ho MC, Lo AC, Kurihara H, Yu AC, Chung SS, Chung SK (2001) Endothelin-1 protects astrocytes from hypoxic/ischemic injury. FASEB J. 15:618-26.

(33) Leri A, Claudio PP, Li Q, Wang X, Reiss K, Wang S, Malhotra A, Kajstura J, Anversa P (1998) Stretch-mediated release of angiotensin II induces myocyte apoptosis by activating p53 that enhances the local renin-angiotensin system and decreases the Bcl-2-to-Bax protein ratio in the cell. J. Clin. Invest. 101:1326–1342.

(34) Li D, Tomson K, Yang B, Mehta P, Croker BP, Mehta JL (1999) Modulation of constitutive nitric oxide synthase, bcl-2 and Fas expression in cultured human coronary endothelial cells exposed to anoxia-reoxygenation and angiotensin II: role of AT1 receptor activation. Cardiovasc. Res. 41:109–115.

(35) Diep QN, Li JS, Schiffrin EL (1999) In vivo study of AT(1) and AT(2) angiotensin receptors in apoptosis in rat blood vessels. Hypertension 34: 617–624.

(36) Li HL, Kostulas N, Huang YM, Xiao BG, van der Meide P, Kostulas V, Giedraitas V, Link H (2001) IL-17 and IFN-gamma mRNA expression is increased in the brain and systemically after permanent middle cerebral artery occlusion in the rat. J. Neuroimmunol. 116:5-14.

(37) Kleinschnitz C, Schroeter M, Jander S, Stoll G (2004) Induction of granulocyte colony-stimulating factor mRNA by focal cerebral ischemia and cortical spreading depression. Brain Res. Mol. Brain Res. 131:73-78.

(38) Arumugam TV, Granger DN, Mattson MP (2005) Stroke and T-cells. Neuromolecular Med. 7: 229-242.

(39) Gorina R, Petegnief V, Chamorro A, Planas AM (2005) AG490 prevents cell death after exposure of rat astrocytes to hydrogen peroxide or proinflammatory cytokines: involvement of the Jak2/ STAT pathway. J. Neurochem. 92:505-518.

(40) Park KW, Lee DY, Joe EH, Kim SU, Jin BK (2005) Neuroprotective role of microglia expressing interleukin-4. J. Neurosci. Res. 81:397-402.

(41) Vitkovic L, Chatham JJ, da Cunha A (1995) Distinct expressions of three cytokines by IL-1-stimulated astrocytes in vitro and in AIDS brain. Brain Behav. Immun. 9:378-88.

(42) Stanimirovic D, Zhang W, Howlett C, Lemieux P, Smith C (2001) Inflammatory gene transcription in human astrocytes exposed to hypoxia: roles of the nuclear factor- kappaB and autocrine stimulation. J. Neuroimmunol. 119:365-76.

(43) Ringheim GE (1995) Mitogenic effects of interleukin-5 on microglia. Neurosci. Lett. 201:131-134.

(44) Benveniste EN, Whitaker JN, Gibbs DA, Sparacio SM, Butler JL (1989) Human B cell growth factor enhances proliferation and glial fibrillary acidic protein gene expression in rat astrocytes. Int. Immunol. 1:219-28.

(45) Merrill JE, Kono DH, Clayton J, Ando DG, Hinton DR, Hofman FM. (1992) Inflammatory leukocytes and cytokines in the peptide-induced disease of experimental allergic encephalomyelitis in SJL and B10.PL mice. Proc. Natl. Acad. Sci. U S A. 89: 574-578.

(46) (46) Fernandes A, Falcao AS, Silva RF, Gordo AC, Gama MJ, Brito MA, Brites D. (2006) Inflammatory signalling pathways involved in astroglial activation by unconjugated bilirubin. J Neurochem. 96:1667-1679.

Figure 1

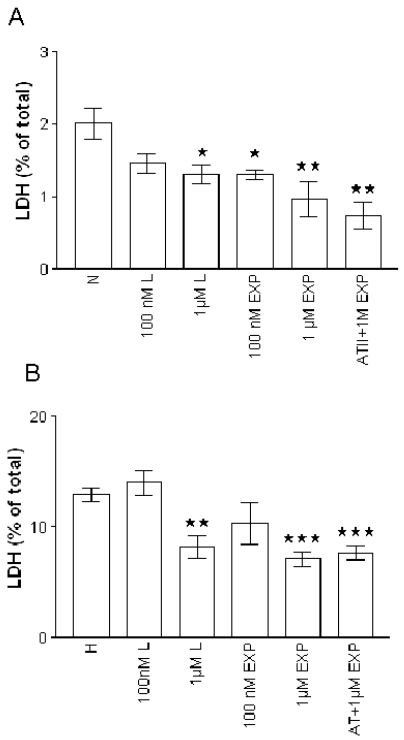

Figure 1. LDH-release from APCs under NC (A) and HC (B). Losartan applied under NC reduced the release of LDH in a concentration-dependent manner in comparison to control culture (Fig.1A: N vs. 100nM L or 1µM L). Both concentrations of EXP3174 (100nM and 1µM, Fig 1 A) and its simultaneous application with 100nM ATII led to a significant LDH-decrease (AT +1µM EXP in Fig.1A). Under HC (Fig.1B) both, losartan and EXP3174 applied in concentration of 100nM brought no changes in released LDH amount. 1µM losartan or EXP3174 and 100nM AT together with EXP3174 significantly reduced hypoxia-induced cytotoxicity (cf. 1µM L, 1µM EXP and AT+1µM EXP with control H in Fig.1B).

Figure 2

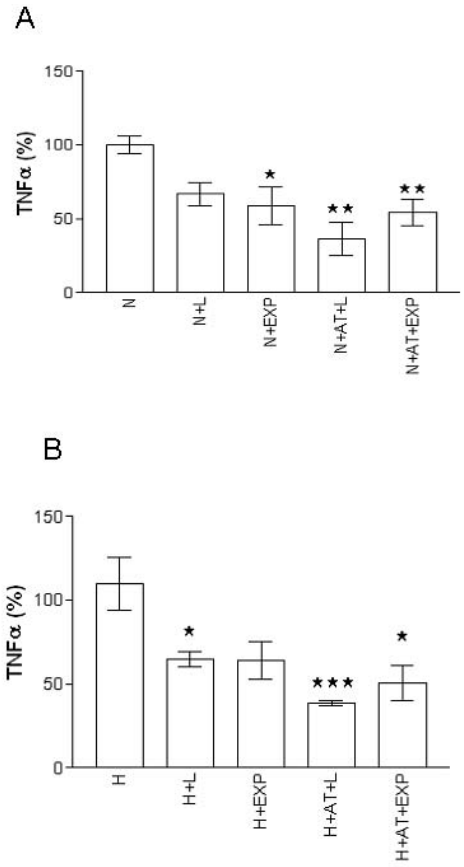

Figure 2. TNFα quantification in APCs under NC (A) and HC (B). The quantification of TNFα revealed a 3,5-fold increase in TNFα-concentration in cell cultures exposed to hypoxia (cf. N in Fig.2A with H in Fig.2B). Under NC (Fig. 2A) losartan and EXP3174 decreased the TNFα-release with an equal potency, whereas under HC the effect of EXP3174 on TNFα-release was considered as insignificant due to a high variability of the data within the treated group (Fig.2B H+EXP). Simultaneous application of ATII with EXP3174 or losartan enhanced the significance of TNFα-reducing effect in NC (Fig.2A, N+AT+L and N+AT+EXP) and HC (Fig. 2B, H+AT+L and H+AT+EXP).

Curriculum Vitae

Name:	Sumaira Umbreen
Date of Birth:	11 June 1974
Place of Birth:	Bahawalnagar, Pakistan
Nationality:	Pakistani
Marital status:	Married
Permanent Address:	Asif Elysium, Shadman colony, Bahawalnagar, Pakistan

Academic career

April 1992 – September 1994	**BSc** in Chemistry, Botany, and Zoology, Institution: University of the Punjab, Pakistan
October 1995 – December 1997	**MSc** Specialized in Organic Chemistry Institution: University of the Punjab, Pakistan **Thesis:** Development of irridescent colours on glass, ceramic and other related materials.
February 1998 – April 2000	**M.Phil.** in Organic Chemistry Institution: Quaid-i-Azam University, Pakistan **Thesis**: Synthesis and reactions of medicinally important heterocycles.
Since October 2002	Doctoral thesis under the supervision of Prof. Dr. Boris Schmidt at Technical University Darmstadt, Germany
Since October 2002	Scientific co-worker at Department of Chemistry and Biochemistry, TU-Darmstadt

Language proficiencies

English, Urdu, Punjabi, German (bridging level), Arabic (basic understanding)

Eidesstattliche Erklärung

Ich erkläre hiermit an Eides statt, dass ich meine Dissertation selbstständig und nur mit den angegebenen Hilfsmitteln angefertigt und noch keinen Promotionsversuch unternommen habe.

Sumaira Umbreen
Darmstadt, den